FEM Analysis of Deformation and Fracture of Polysynthetically-twinned γ-TiAl + α_2-Ti_3Al Intermetallics

MS Thesis

Surya Batchu

Department of Mechanical Engineering, Clemson University

OUTLINE

- Use of γ-TiAl + α_2-Ti_3Al Alloys in High-Temperature Structural Applications
- Crystal Structures and Slip Systems in γ-TiAl and α_2-Ti_3Al
- Polysynthetically-Twinned γ-TiAl + α_2-Ti_3Al Single Crystals
- Crystal Plasticity Formulation
- Determination of Crystal-Plasticity Parameters for γ-TiAl and α_2-Ti_3Al Single Crystals
- Determination of Crystal-Plasticity Parameters for Polysynthetically-Twinned γ-TiAl + α_2-Ti_3Al Single Crystals
- Integration of the Material State
- FEM Modeling of Deformation and Fracture in Polycrystalline γ-TiAl + α_2-Ti_3Al Single Crystals

Use of

γ-TiAl + α_2-Ti_3Al Alloys

in High-Temperature

Structural Applications

Favorable High-Temperature Properties:

- **Excellent Creep Resistance**
- **Excellent Oxidation Resistance**
- **Light Weight**

Limitations to Applications:

- **Low Ambient-Temperature Ductility**
- **Low Ambient-Temperature Fracture Toughness (K_{IC}< 30 MPa$\sqrt{m}$)**

Crystal Structures

and

Slip Systems

in

γ-TiAl and α_2-Ti_3Al

$L1_o$ γ-TiAl Structure

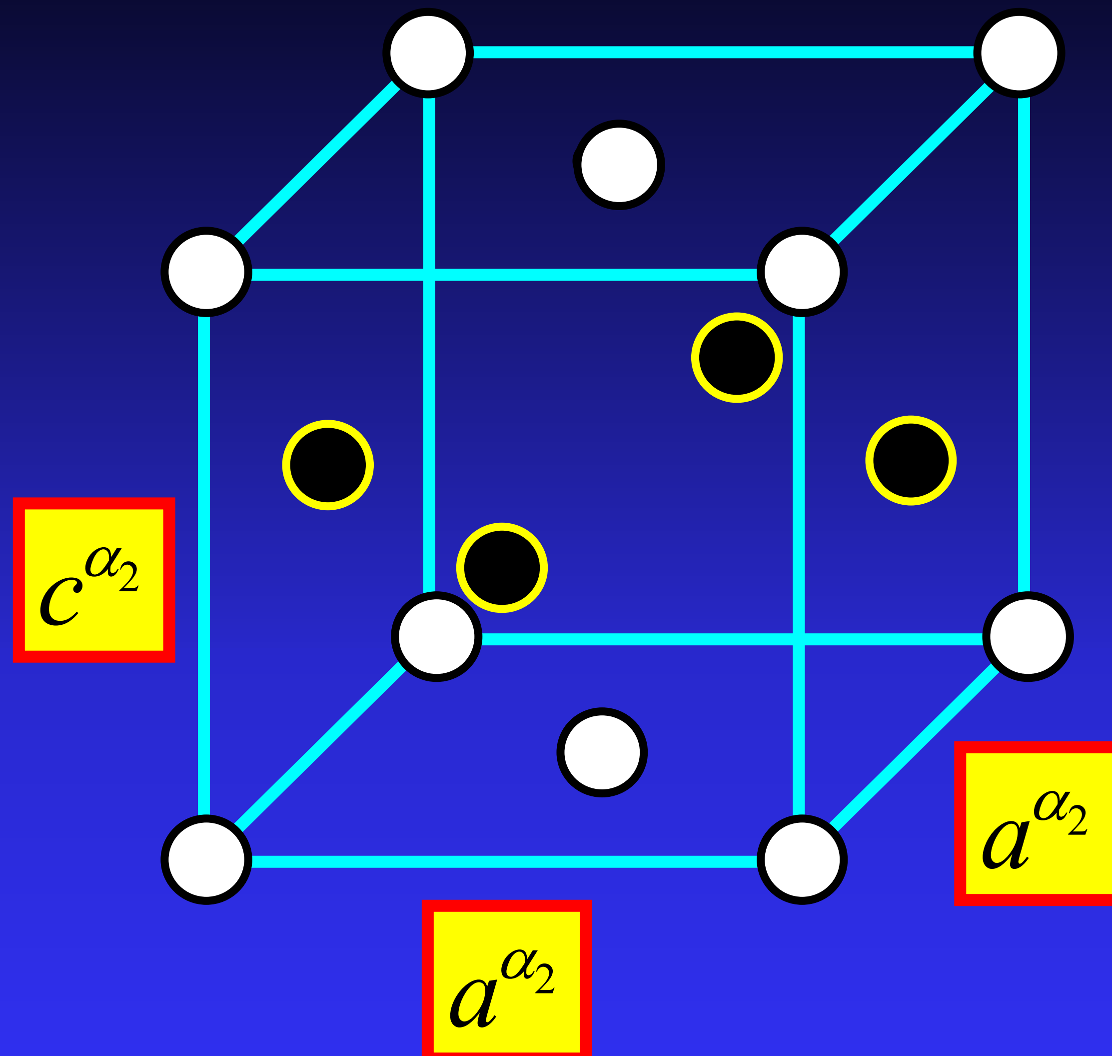

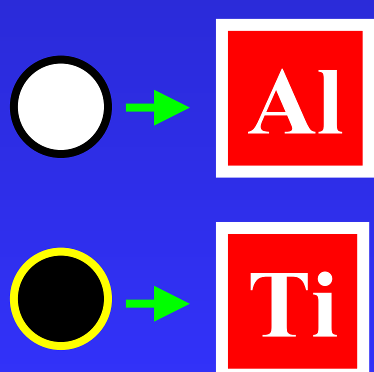

DO_{19}
α_2-Ti_3Al Structure

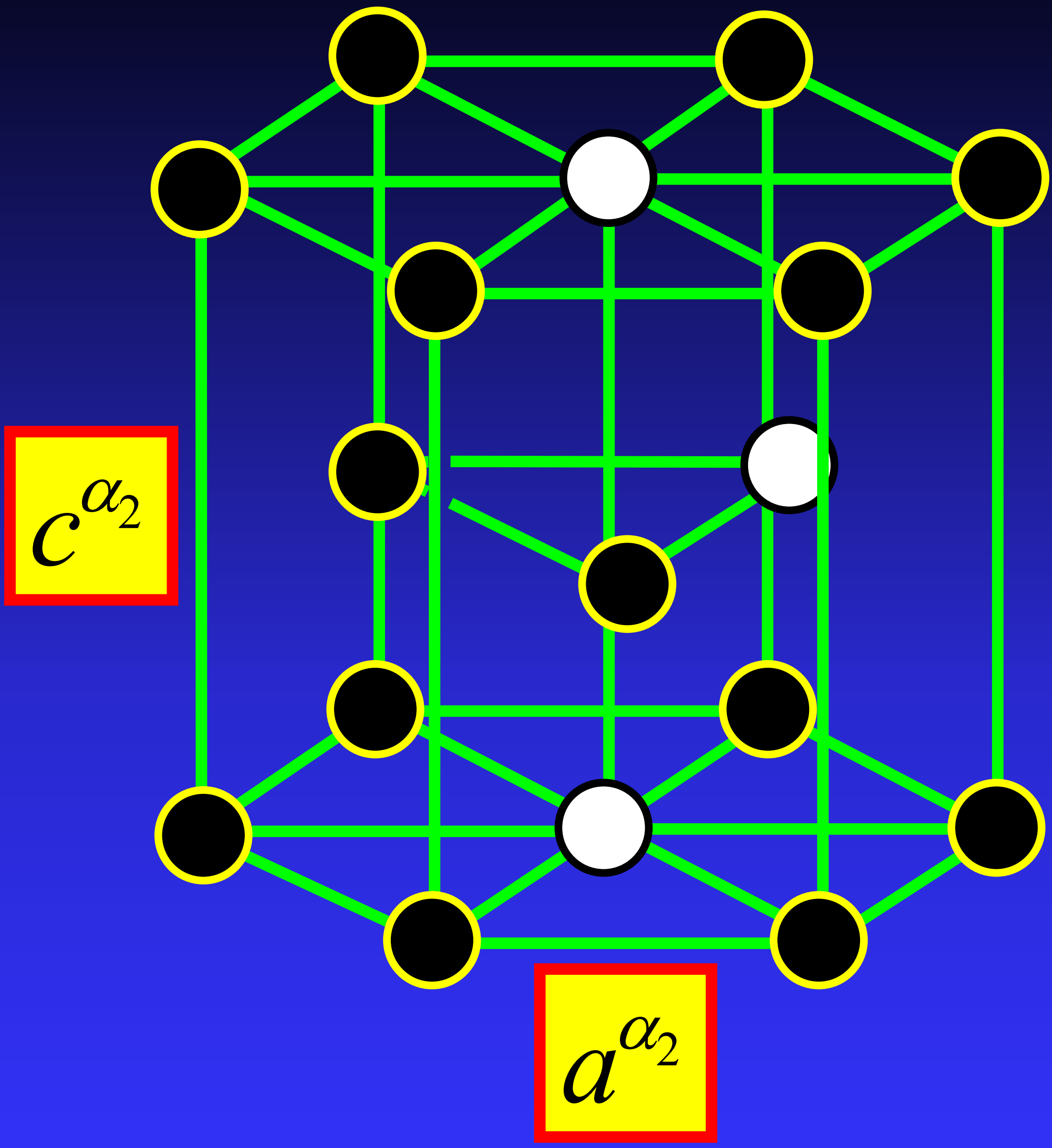

○ → Al

● → Ti

γ-TiAl

Bases:
Orthogonal
Orthonormal
Lattice Parameters

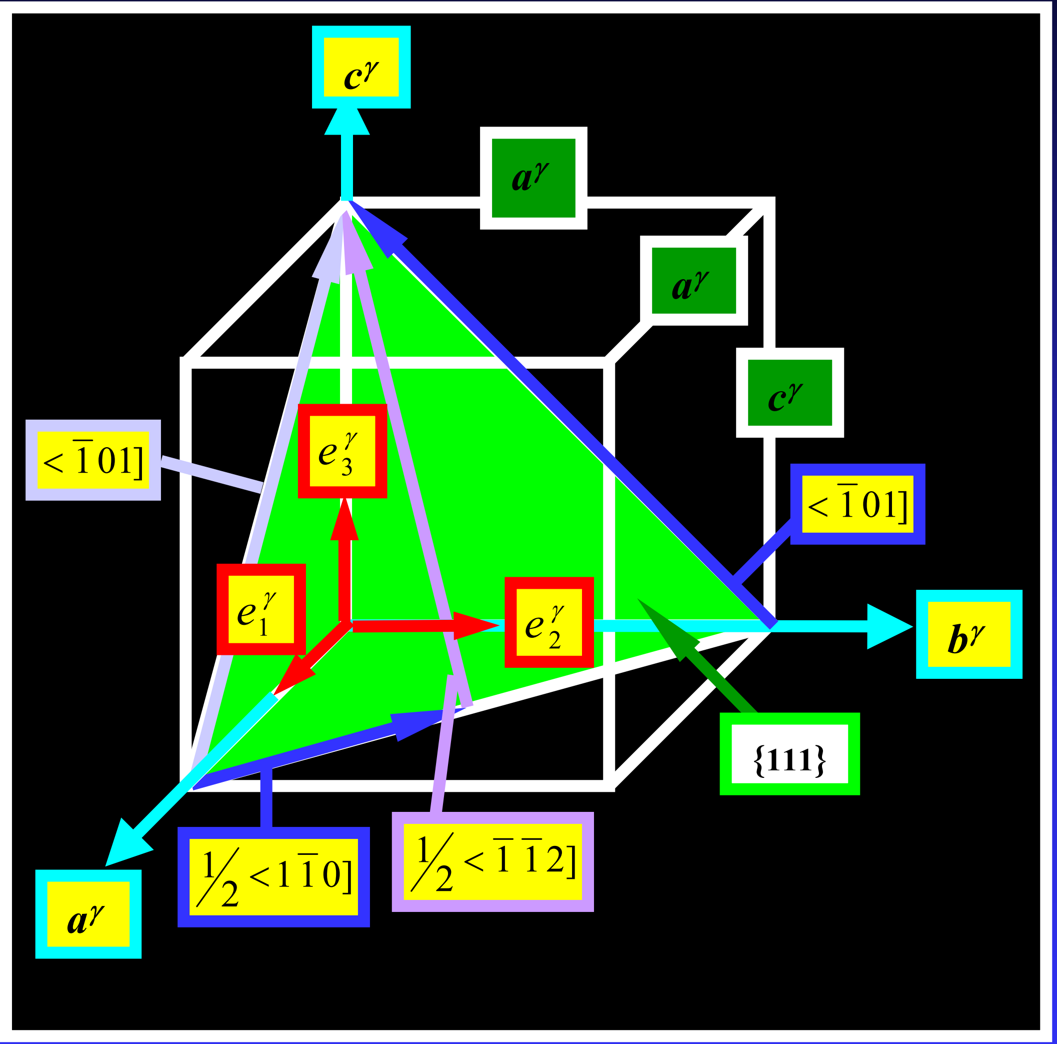

Active Slip Systems:

$<110]\{111\}$
and $<10\bar{1}]\{111\}$

HCP Cell

Simple Hexagonal
Ortho-Hexagonal
Hexagonal Prism

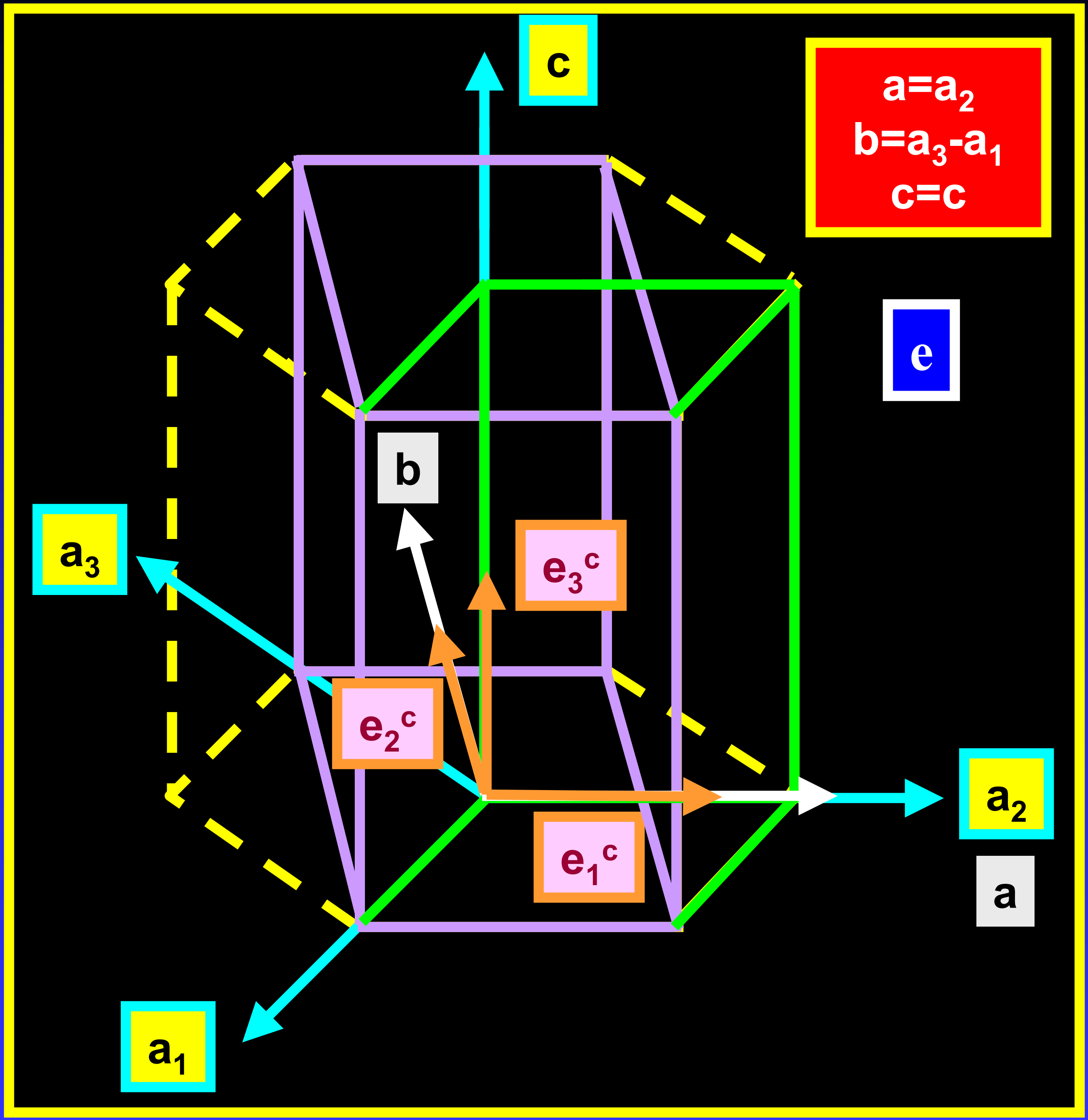

α_2-Ti_3Al

Simple Hexagonal
Ortho-Hexagonal
Hexagonal Prism

Prismatic Slip Systems

$\{10\bar{1}0\} < 1\bar{2}10 >$

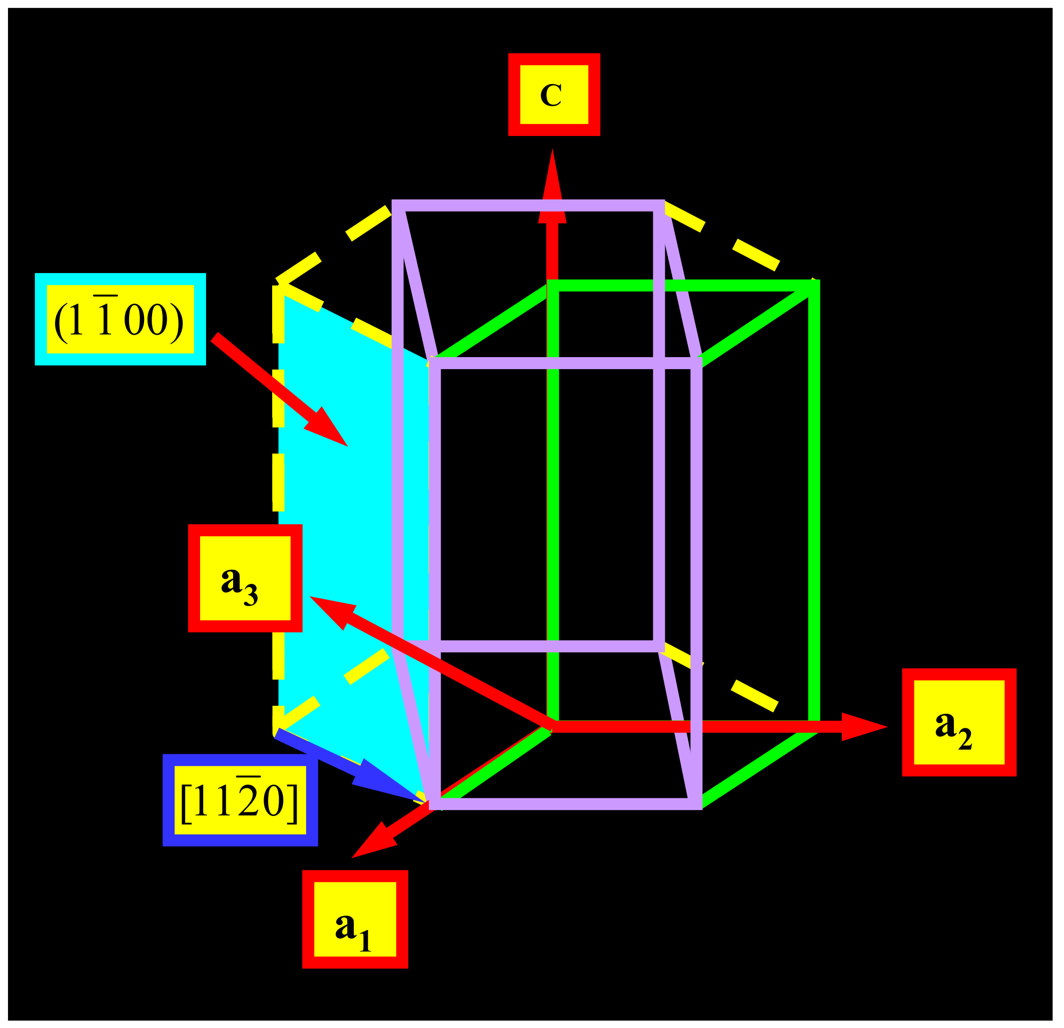

Simple Hexagonal

Ortho-Hexagonal

Hexagonal Prism

α_2-Ti_3Al

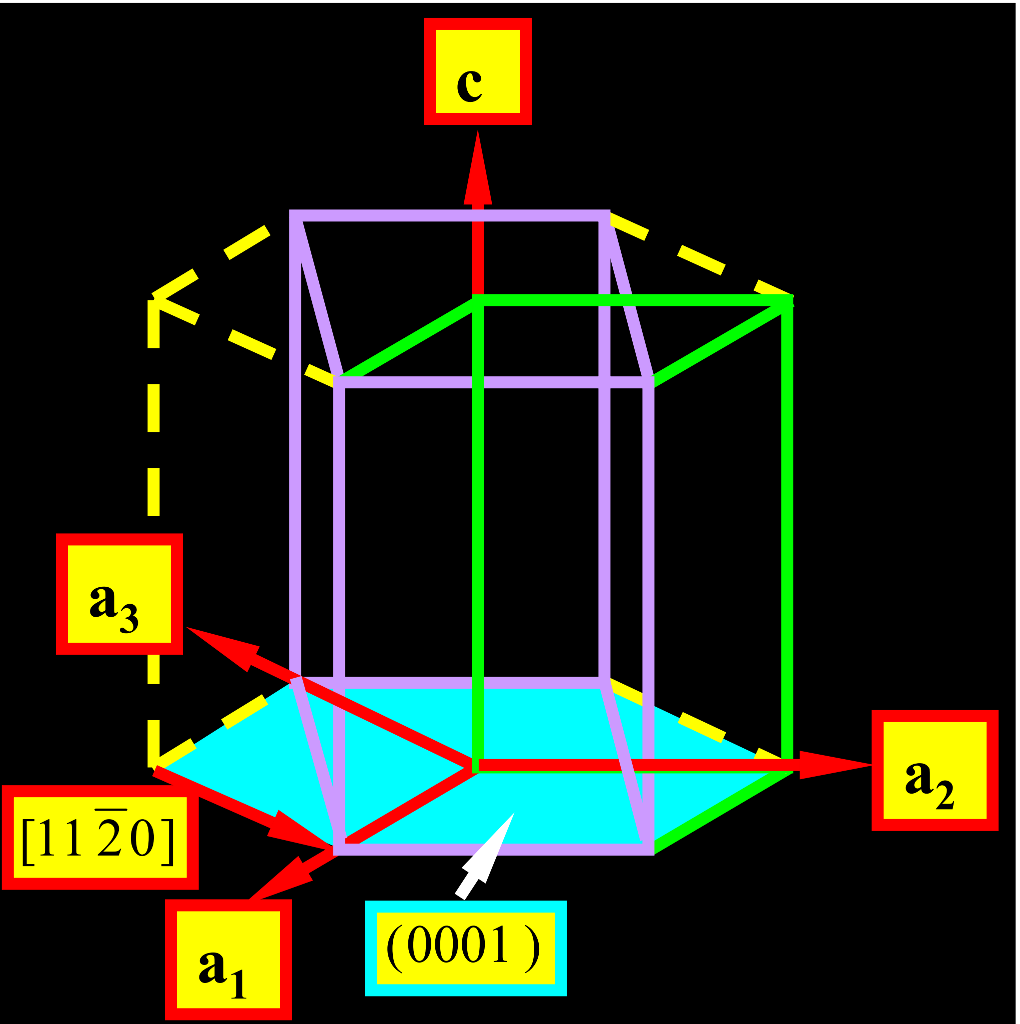

Basal

$(0001)<11\bar{2}0>$

Slip Systems

Simple Hexagonal

Ortho-Hexagonal

Hexagonal Prism

α_2-Ti_3Al

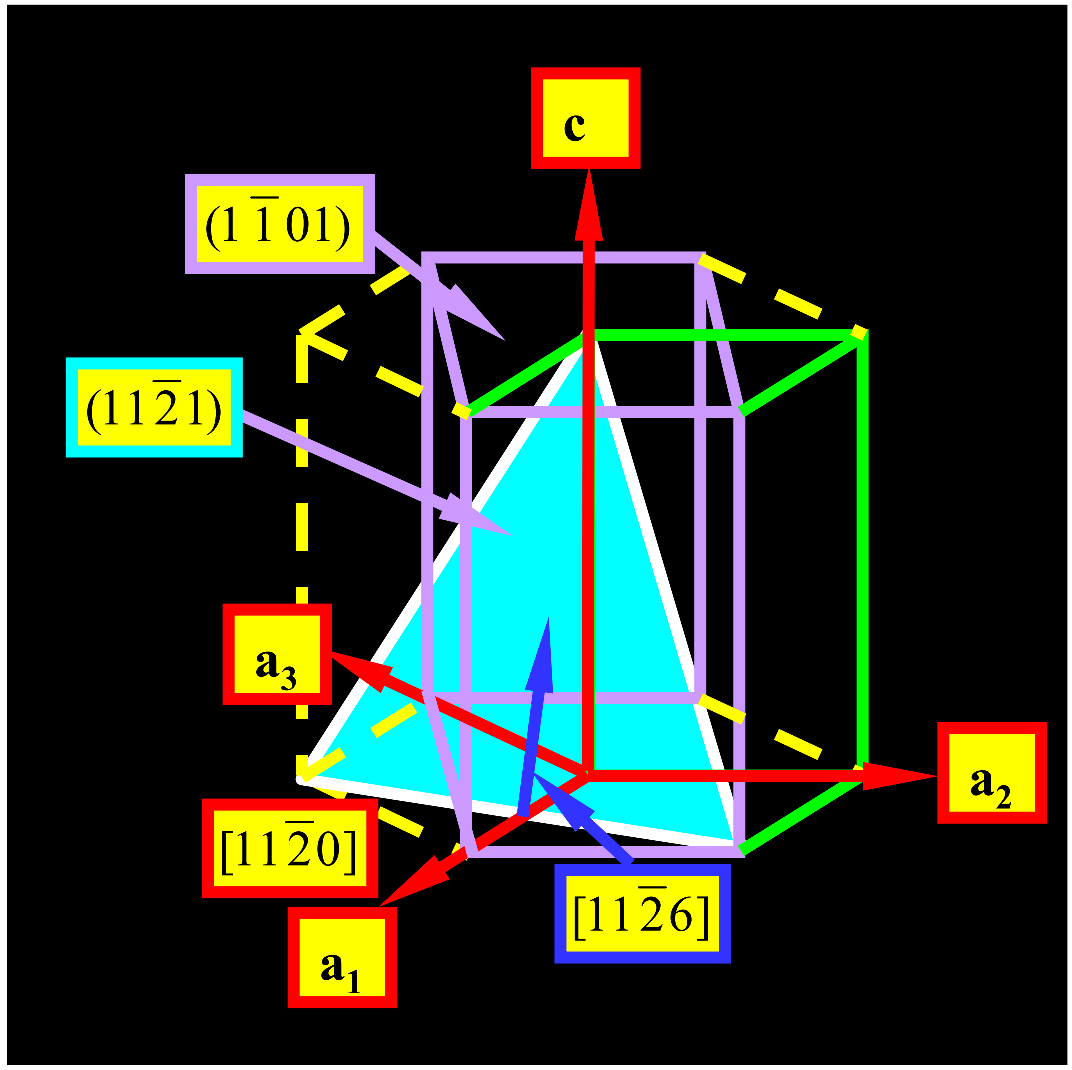

Pyramidal

$\{11\bar{2}1\}<11\bar{2}6>$

Slip Systems

Polysynthetically-

Twinned

γ-TiAl + α_2-Ti_3Al

Single Crystals

Polysynthetically-twinned γ-TiAl+α_2-Ti_3Al Single Crystals

$$\{1\,1\,1\}_{\gamma} \parallel (0\,0\,0\,1)_{\alpha_2}$$

$$<1\,\bar{1}\,0]_{\gamma} \parallel <1\,1\,\bar{2}\,0>_{\alpha_2}$$

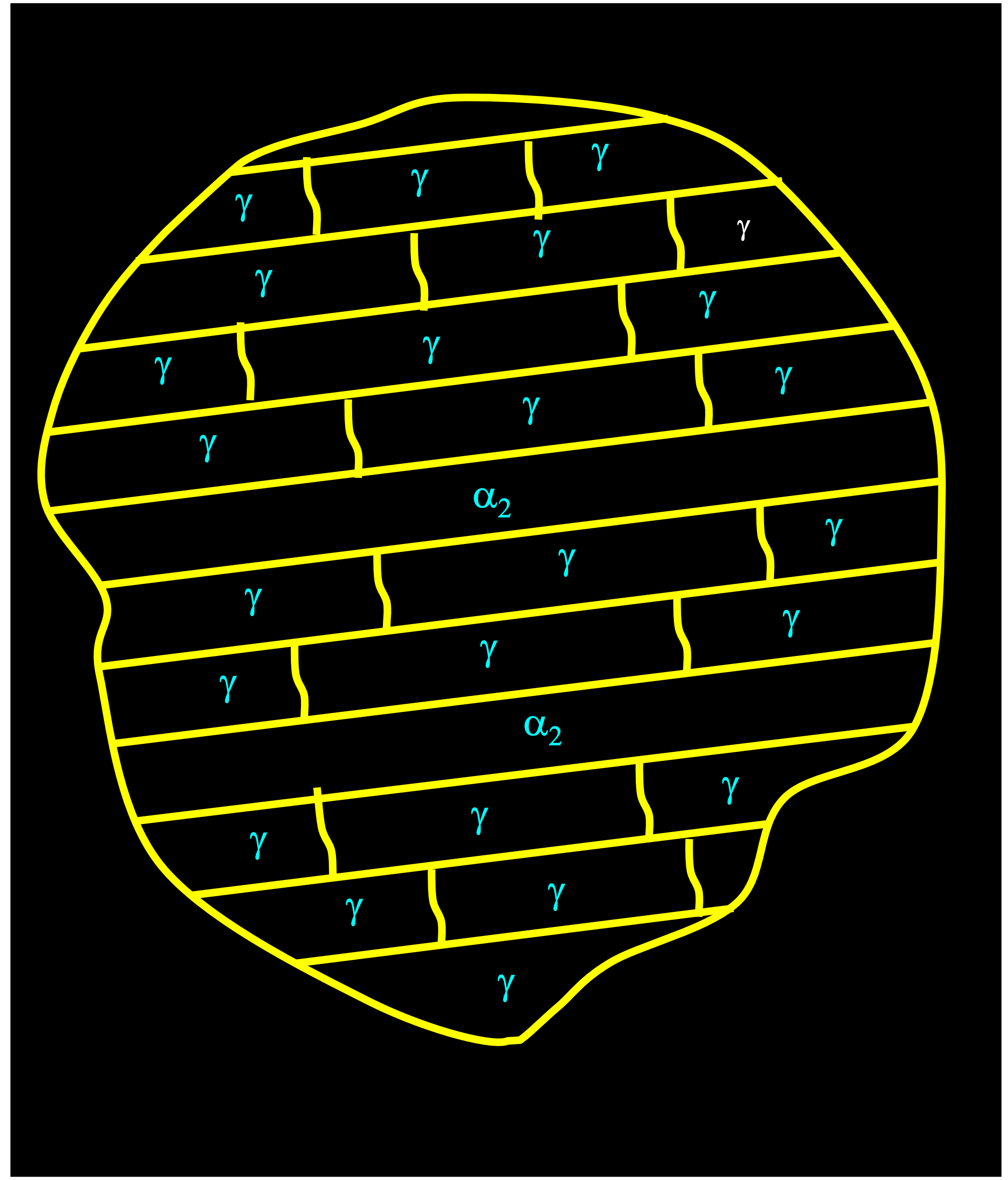

Crystal Plasticity Formulation

Materials Constitutive Model

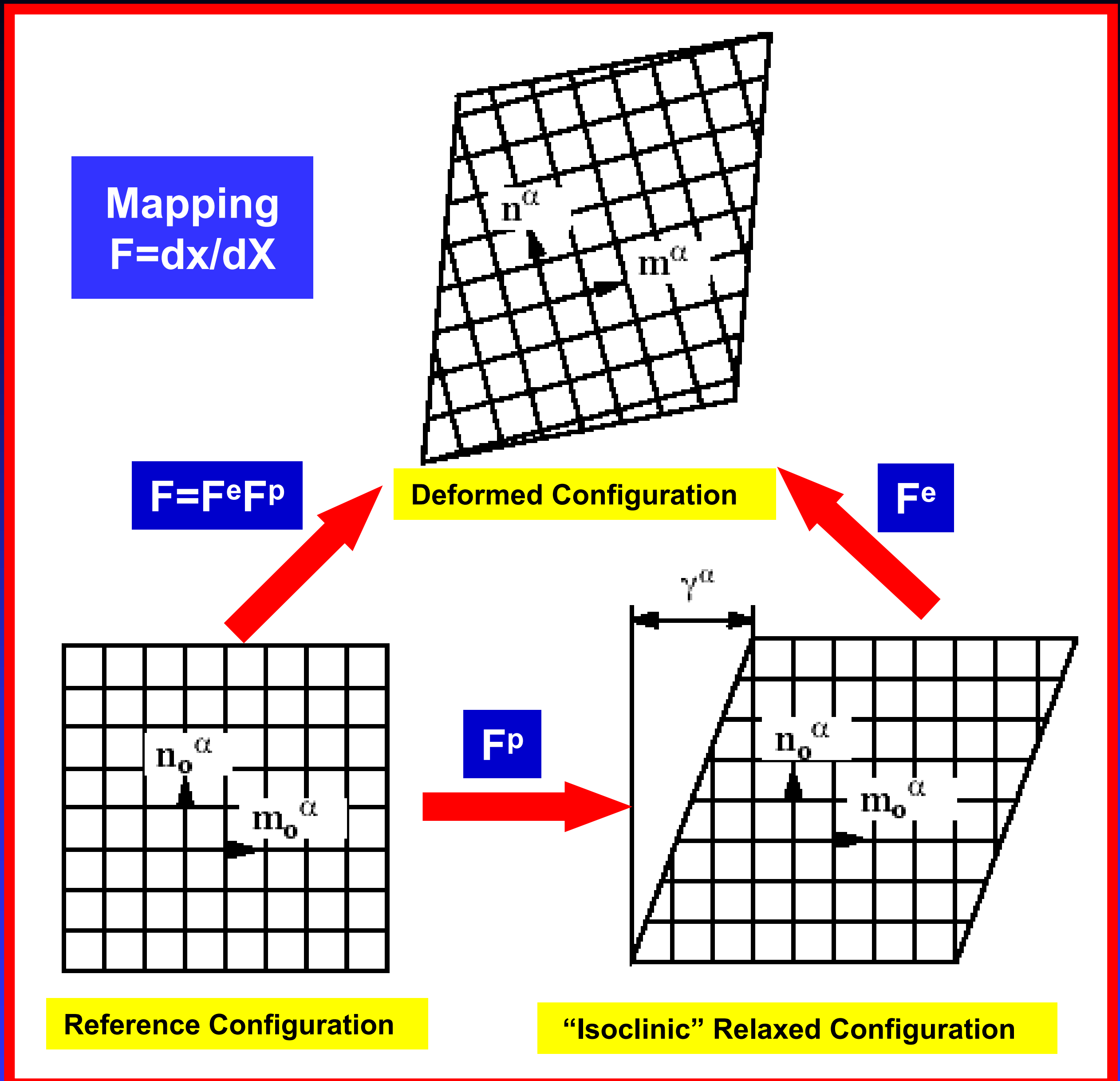

Materials Constitutive Model, cont'd.

Multiplicative Decomposition of Deformation Gradient

$$F^e \equiv F F^{p-1} \quad , \qquad \det F^e > 0$$

Stress vs. Strain Relationship

$$T^* = C[E^e]$$

Stress and Strain Definitions

$$E^e \equiv (1/2)\left\{F^{eT} F^e - I\right\} \qquad\qquad T^* \equiv (\det F^e) F^{e-1} T F^{e-T}$$

Materials Constitutive Model, cont'd.

Elasticity Tensor for γ-TiAl Phase

Six Independent Non-Zero Components

$C_{11}=C_{22}$, C_{33}, C_{12}, $C_{13}=C_{23}$, $C_{44}=C_{55}$, C_{66}

Elasticity Tensor for α_2-Ti_3Al Phase

Six Different (Five Independent) Non-Zero Components

$C_{11}=C_{22}$, C_{33}, C_{12}, $C_{23}=C_{13}$, $C_{44}=C_{55}$,

$C_{66}=0.5(C_{11}-C_{12})$

Materials Constitutive Model, cont'd.

Definition of Slip Plane Normal and Slip Direction Components

For a {h k l} <u v w> slip system in γ-TiAl

$$\{n^{\alpha}_{0,1}, n^{\alpha}_{0,2}, n^{\alpha}_{0,3}\} = \{h / a^{\gamma}, k / a^{\gamma}, l / a^{\gamma}\} / \left| \{h / a^{\gamma}, k / a^{\gamma}, l / a^{\gamma}\} \right|;$$

$$< m^{\alpha}_{0,1}, m^{\alpha}_{0,2}, m^{\alpha}_{0,3} > = < ua^{\gamma}, va^{\gamma}, wa^{\gamma} > / \left| < ua^{\gamma}, va^{\gamma}, wa^{\gamma} > \right|.$$

For a {h k m l} <u v z w> slip system in α_2-Ti_3Al

$$\{n^{\alpha}_{0,1}, n^{\alpha}_{0,2}, n^{\alpha}_{0,3}\} = \{k, -(k+2h)/\sqrt{3}, l/(c^{\alpha 2}/a^{\alpha 2})\} / \left| \{k, -(k+2h)/\sqrt{3}, l/(c^{\alpha 2}/a^{\alpha 2})\} \right|;$$

$$< m^{\alpha}_{0,1}, m^{\alpha}_{0,2}, m^{\alpha}_{0,3} > = < 3v/2, -\sqrt{3}(u+v/2), w(c^{\alpha 2}/a^{\alpha 2}) > / \left| < 3v/2, -\sqrt{3}(u+v/2), w(c^{\alpha 2}/a^{\alpha 2}) > \right|.$$

Materials Constitutive Model, cont'd.

Evolution Equation for Plastic Deformation Gradient

$$\dot{F}^p F^{p-1} = \sum_{\beta} \dot{\gamma}^\alpha S_0^\alpha \qquad S_0^\alpha \equiv m_0^\alpha \otimes n_0^\alpha$$

Shearing Rate on Slip System α

$$\dot{\gamma}^\alpha = \dot{\tilde{\gamma}} \left| \frac{\tau^\alpha}{s^\alpha} \right|^{1/m} \operatorname{sign}\left(\tau^\alpha\right)$$

Resolved Shear Stress

$$\tau^\alpha \equiv T^* \cdot S_o^\alpha$$

Materials Constitutive Model, cont'd.

Shear Resistance Evolution Equation

$$\dot{s}^{\alpha} = \sum_{\beta} h^{\alpha\beta} \left| \dot{\gamma}^{\beta} \right|$$

Hardening Rate Matrix

$$h^{\alpha\beta} = q^{\alpha\beta} h^{\beta}$$

Self Hardening Rate

$$h^{\beta} = h_0^{\beta} \left| 1 - \frac{s^{\beta}}{s_s^{\beta}} \right|^{r} sign\left(1 - \frac{s^{\beta}}{s_s^{\beta}} \right)$$

Materials Constitutive Model, cont'd.

Latent Hardening Rate

$$q^{\alpha\beta} = \begin{cases} 1 & \text{if } \alpha \text{ and } \beta \text{ are coplanar slip systems} \\ q_l & \text{otherwise} \end{cases}$$

Coplanar Slip Systems in the Two Phases

γ - TiAl Phase : One $\{111\} < 1\,\bar{1}\,0]$, two $\{111\} < 0\,\bar{1}\,1]$, one $\{111\}[11\bar{2}]$ slip systems

$\alpha_2 - Ti_3Al$ Phase : Three basal < a > -slip systems : $(0001)[11\bar{2}0]$, $(0001)[\bar{2}110]$, $(0001)[1\bar{2}10]$

Determination of Crystal-Plasticity Parameters for γ-TiAl and α_2-Ti_3Al Single Crystals

Results

Crystallographic Parameters for Five γ-TiAl Single-Crystal Orientations Used in the Work of Kawabata et al.

Orientation of Compression Axis	Slip Systems with Maximum Initial Schmid Factor	Magnitude of Schmid Factor
$[001]$	Eight $<10\bar{1}]\{111\}$	~0.409
$[\bar{1}10]$	Four $<10\bar{1}]\{111\}$	~0.409
$[010]$	Four $<1\bar{1}0]\{111\}$ Four $<10\bar{1}]\{111\}$	~0.409
$\sim[\bar{2}96]$	Single $[1\bar{1}0](111)$	~0.482
$\sim[\bar{2}45]$	Single $[10\bar{1}](111)$	~0.445

Results Cont'd.

γ-TiAl Single Crystals

Curve Fitting

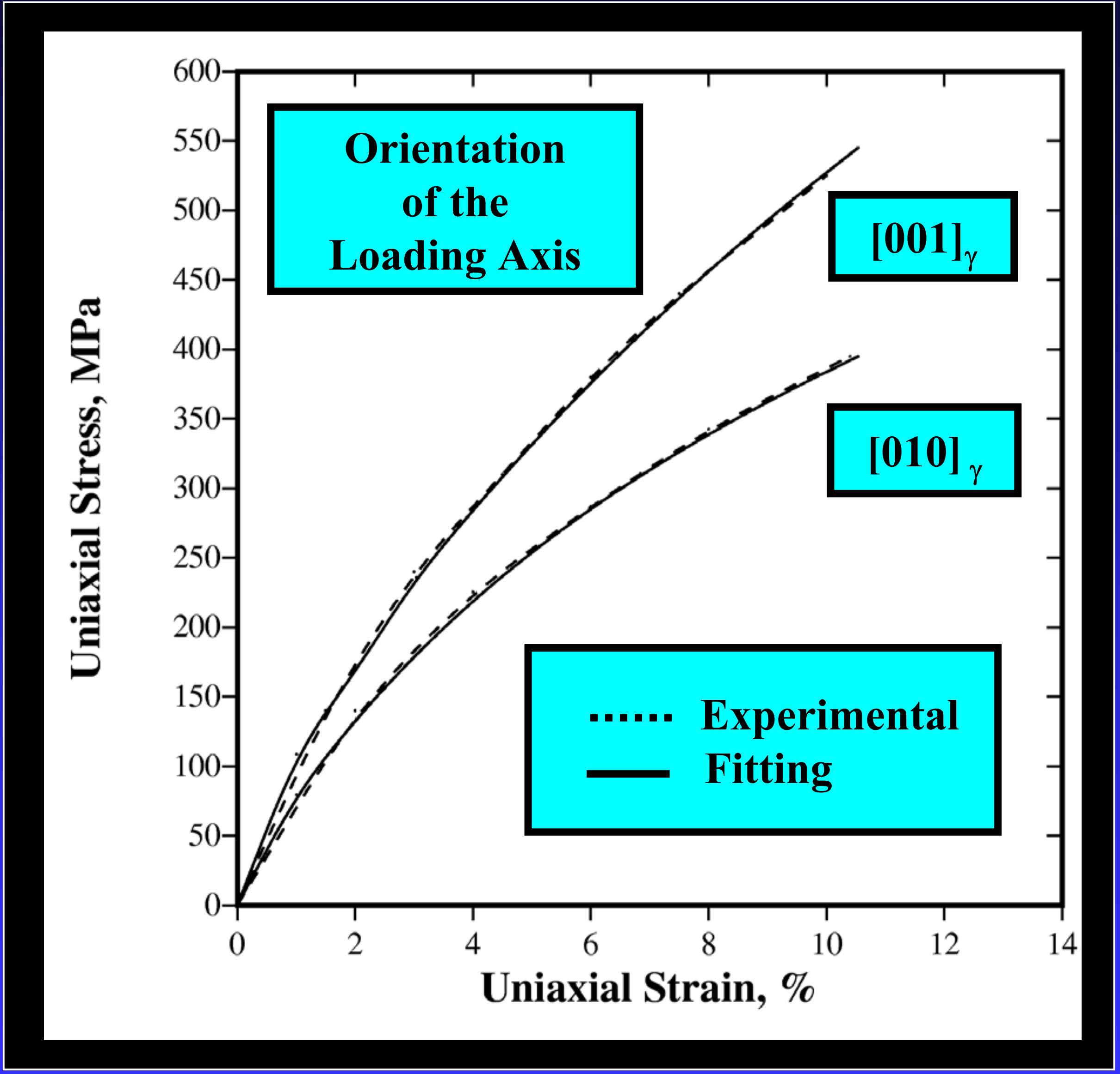

Results Cont'd.

Crystal-Plasticity Parameters for the γ-TiAl Single Crystals

Parameter	Symbol	Value	Units	Reference
Elastic Constant	C_{11}	190	GPa	(22)
Elastic Constant	C_{33}	185	GPa	(22)
Elastic Constant	C_{12}	105	GPa	(22)
Elastic Constant	C_{13}	90	GPa	(22)
Elastic Constant	C_{44}	120	GPa	(22)
Elastic Constant	C_{66}	50	GPa	(22)
Reference Shearing Rate	$\dot{\tilde{\gamma}}_0$	0.005	s^{-1}	This Work
Strain Rate Sensitivity	m	0.014	N/A	This Work
Latent Hardening Parameter	q_l	1.4	N/A	This Work

Table Cont'd. ↓

Results Cont'd.

Table Cont'd.

Self-Hardening Exponent	$\{111\}\ 1/2\langle 1\bar{1}0]$	r	3.1	N/A	This Work
	$\{111\}\ \langle \bar{1}01]$		3.0		
Initial Slip Resistance	$\{111\}\ 1/2\langle 1\bar{1}0]$	s_0	14.3	Mpa	This Work
	$\{111\}\ \langle \bar{1}01]$		22.7		
Self-Hardening Parameter	$\{111\}\ 1/2\langle 1\bar{1}0]$	h_o	940.2	Mpa	This Work
	$\{111\}\ \langle \bar{1}01]$		950.7		
Saturation Slip Resistance	$\{111\}\ 1/2\langle 1\bar{1}0]$	s_s	212.2	MPa	This Work
	$\{111\}\ \langle \bar{1}01]$		291.1		

Results Cont'd.

γ-TiAl Single Crystals

Predicted Curves

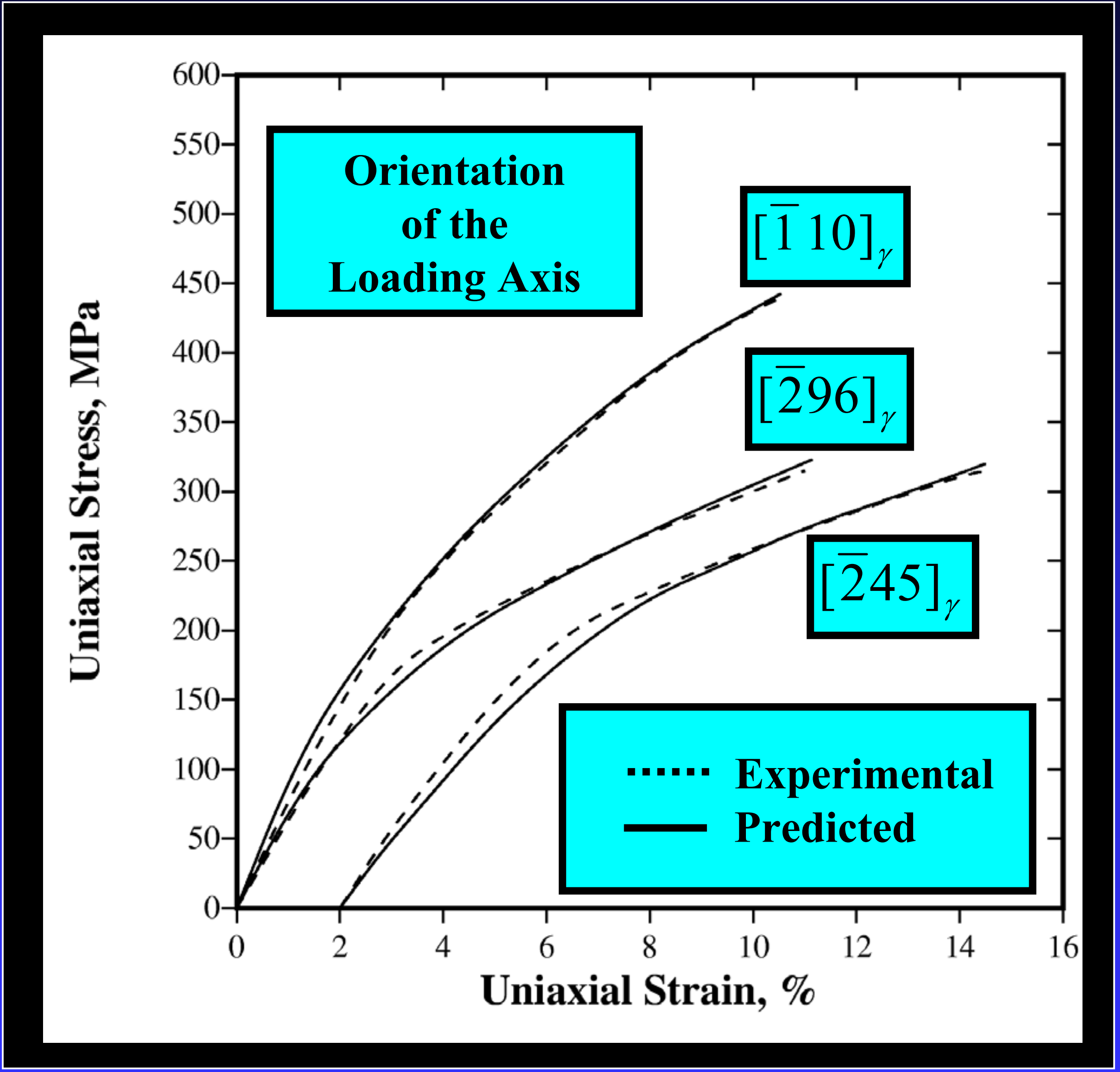

Results

Crystallographic Parameters for the α_2-Ti_3Al Single Crystals Used in the Work of Inui et al.

$\omega = \phi = 0,\ 0 \le \theta \le 90^0$

Single-Crystal Orientation		Magnitude of Schmid Factor		
Orientation of Compression Axis	Euler Angle, θ	$(0001) < 11\bar{2}0 >$ Basal Slip	$(1\bar{1}00) < 11\bar{2}0 >$ Prismatic Slip	$(11\bar{2}1) < \bar{1}\bar{1}26 >$ Pyramidal Slip
$[0001]$	0	0	0	0.4494
$[11\bar{2}4]$	22	0.3449	0.0619	0.4459
$[11\bar{2}2]$	39	0.4889	0.1732	0.3321
$[11\bar{2}1]$	59	0.4454	0.3149	0.3995
$[11\bar{2}0]$	90	0	0.4330	0.4494

Results Cont'd.

α_2-Ti_3Al Single Crystals

Curve Fitting

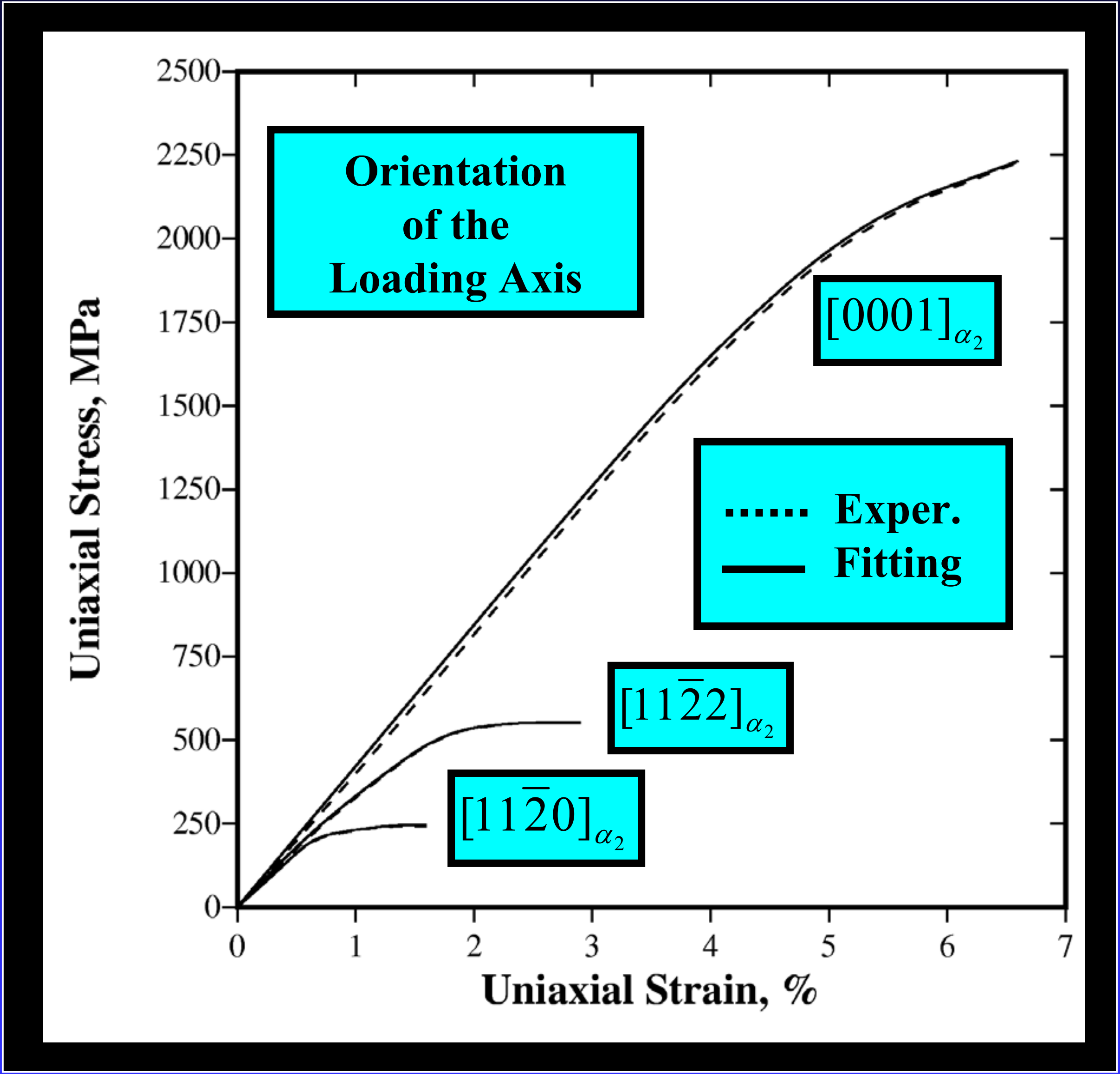

Results Cont'd.

Crystal-Plasticity Parameters for the α_2-Ti_3Al Single Crystals

Parameter	Symbol	Value	Units	Reference
Elastic Constant	C_{11}	221	GPa	(23)
Elastic Constant	C_{33}	238	GPa	(23)
Elastic Constant	C_{12}	71	GPa	(23)
Elastic Constant	C_{13}	85	GPa	(23)
Elastic Constant	C_{44}	69	GPa	(23)
Reference Shearing Rate	$\dot{\tilde{\gamma}}_0$	0.001	s^{-1}	This Work
Strain Rate Sensitivity	m	0.009	N/A	This Work
Latent Hardening Parameter	q_l	1.4	N/A	This Work

Table Cont'd. ↓

Self-Hardening Exponent	$\{1\bar{1}00\}\langle 11\bar{2}0\rangle$	r	2.7	N/A	This Work
	$\{0001\}\langle 11\bar{2}0\rangle$		3.0		
	$\{11\bar{2}1\}\langle 11\bar{2}6\rangle$		2.9		
Initial Slip Resistance	$\{1\bar{1}00\}\langle 11\bar{2}0\rangle$	s_0	19.2	MPa	This Work
	$\{0001\}\langle 11\bar{2}0\rangle$		44.8		
	$\{11\bar{2}1\}\langle 11\bar{2}6\rangle$		121.9		
Self-Hardening Parameter	$\{1\bar{1}00\}\langle 11\bar{2}0\rangle$	h_o	861.7	MPa	This Work
	$\{0001\}\langle 11\bar{2}0\rangle$		742.8		
	$\{11\bar{2}1\}\langle 11\bar{2}6\rangle$		814.7		
Saturation Slip Resistance	$\{1\bar{1}00\}\langle 11\bar{2}0\rangle$	s_s	149.3	MPa	This Work
	$\{0001\}\langle 11\bar{2}0\rangle$		417.7		
	$\{11\bar{2}1\}\langle 11\bar{2}6\rangle$		1586.3		

Results Cont'd.

α_2-Ti_3Al Single Crystals

Predicted Curves

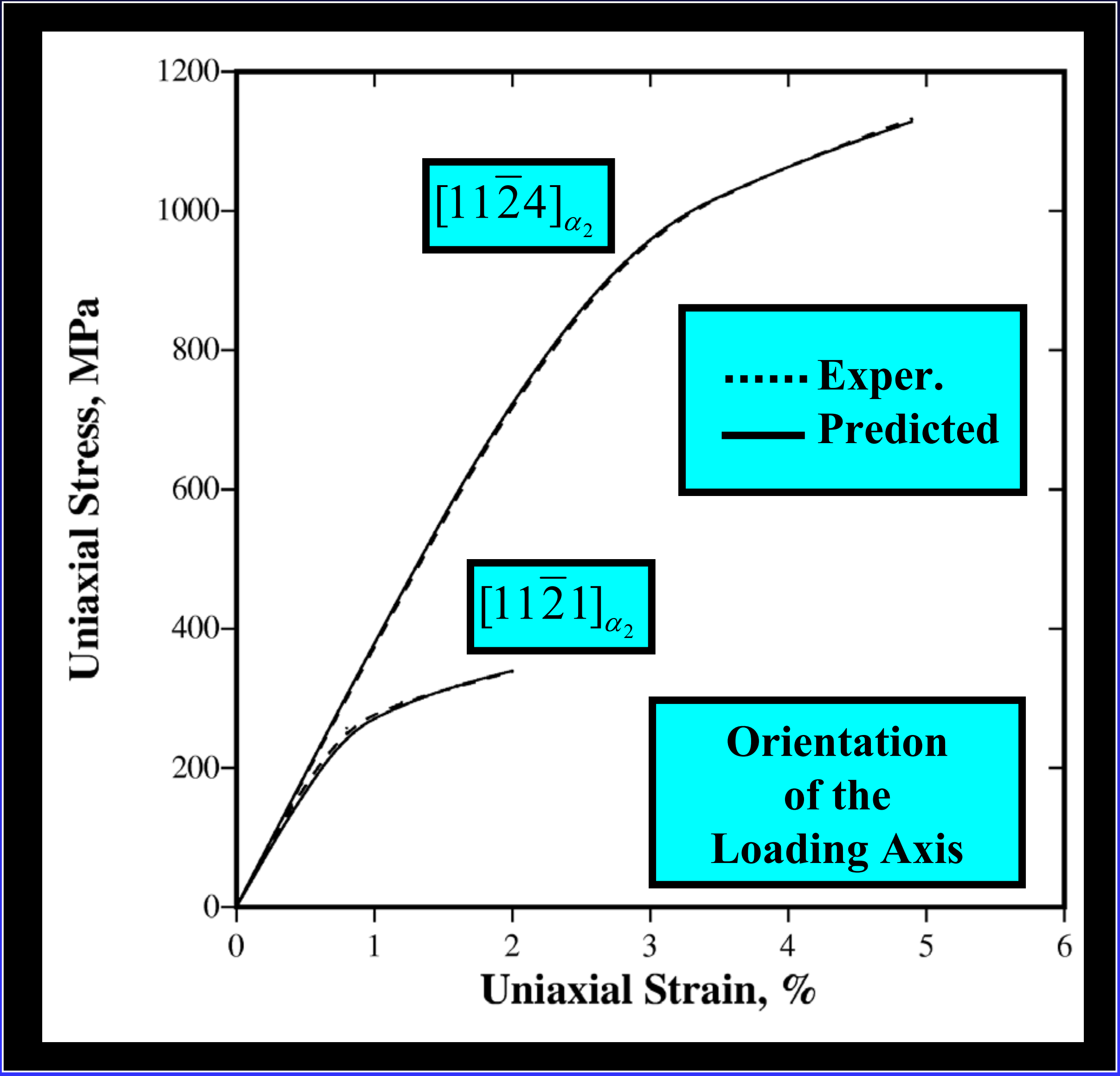

Determination of Crystal-Plasticity Parameters for Polysynthetically-Twinned γ-TiAl + α_2-Ti_3Al Single Crystals

Results Cont'd.

γ-TiAl + α_2-Ti_3Al Single Crystals

Slip System	Symbol	Slip Type
$[1\bar{1}0](111)$	S1	Soft Mode
$[\bar{1}01](111)$		
$[01\bar{1}](111)$		
$[\bar{1}01](1\bar{1}1)$	S2	Soft Mode
$[1\bar{1}0](11\bar{1})$		
$[0\bar{1}1](\bar{1}11)$		

Table Cont'd. ↓

Results Cont'd.

γ-TiAl + α_2-Ti_3Al Single Crystals

	H1	Hard Mode
$[1\bar{1}0](111)$		
$[\bar{1}01](111)$		
$[01\bar{1}](111)$		
$[\bar{1}01](1\bar{1}1)$		
$[1\bar{1}0](11\bar{1})$		
$[0\bar{1}1](\bar{1}11)$		

Results Cont'd.

γ-TiAl + α_2-Ti_3Al Single Crystals

Curve Fitting

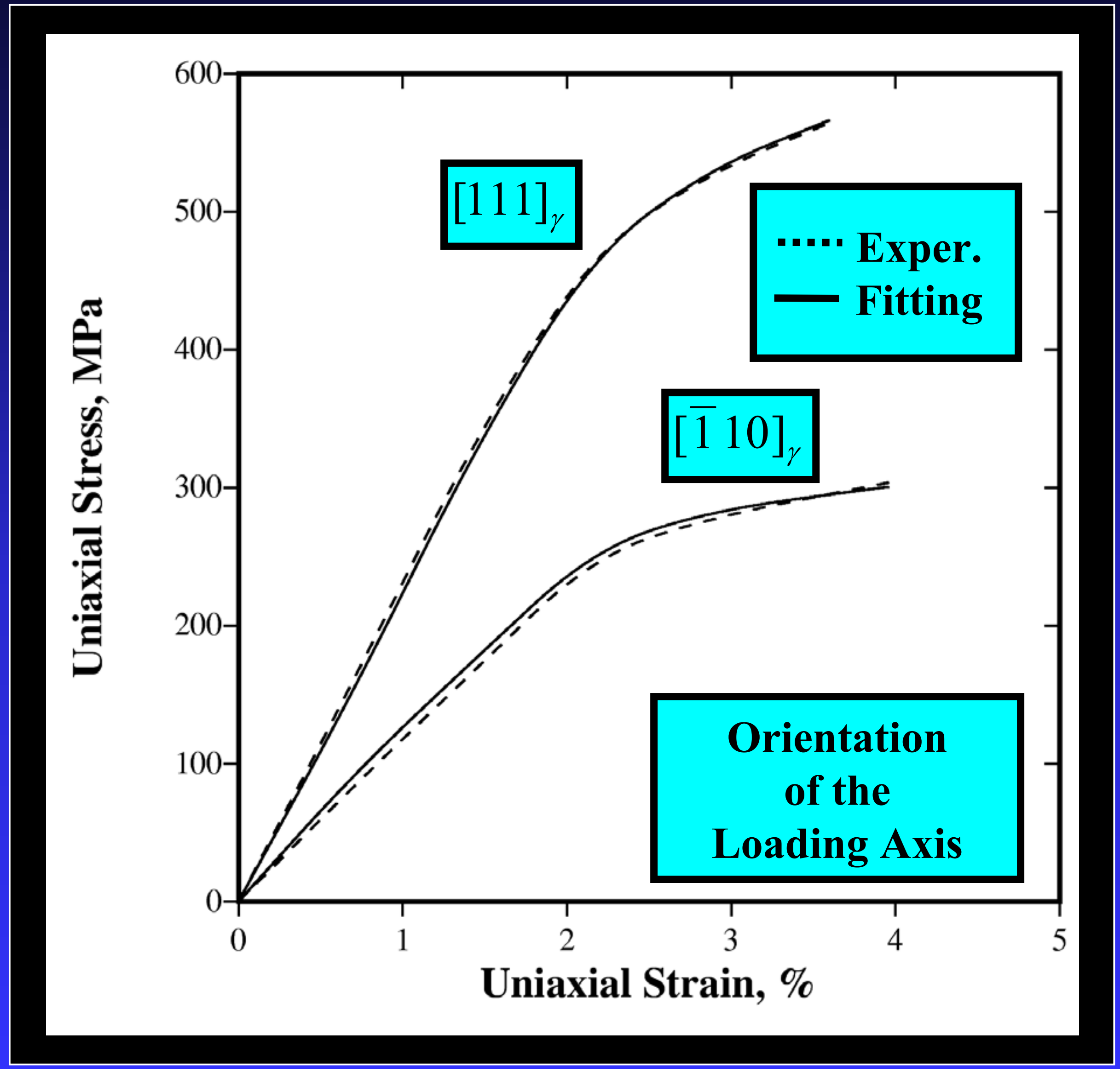

Results Cont'd.

γ-TiAl + α_2-Ti_3Al Single Crystals

Predicted Curves

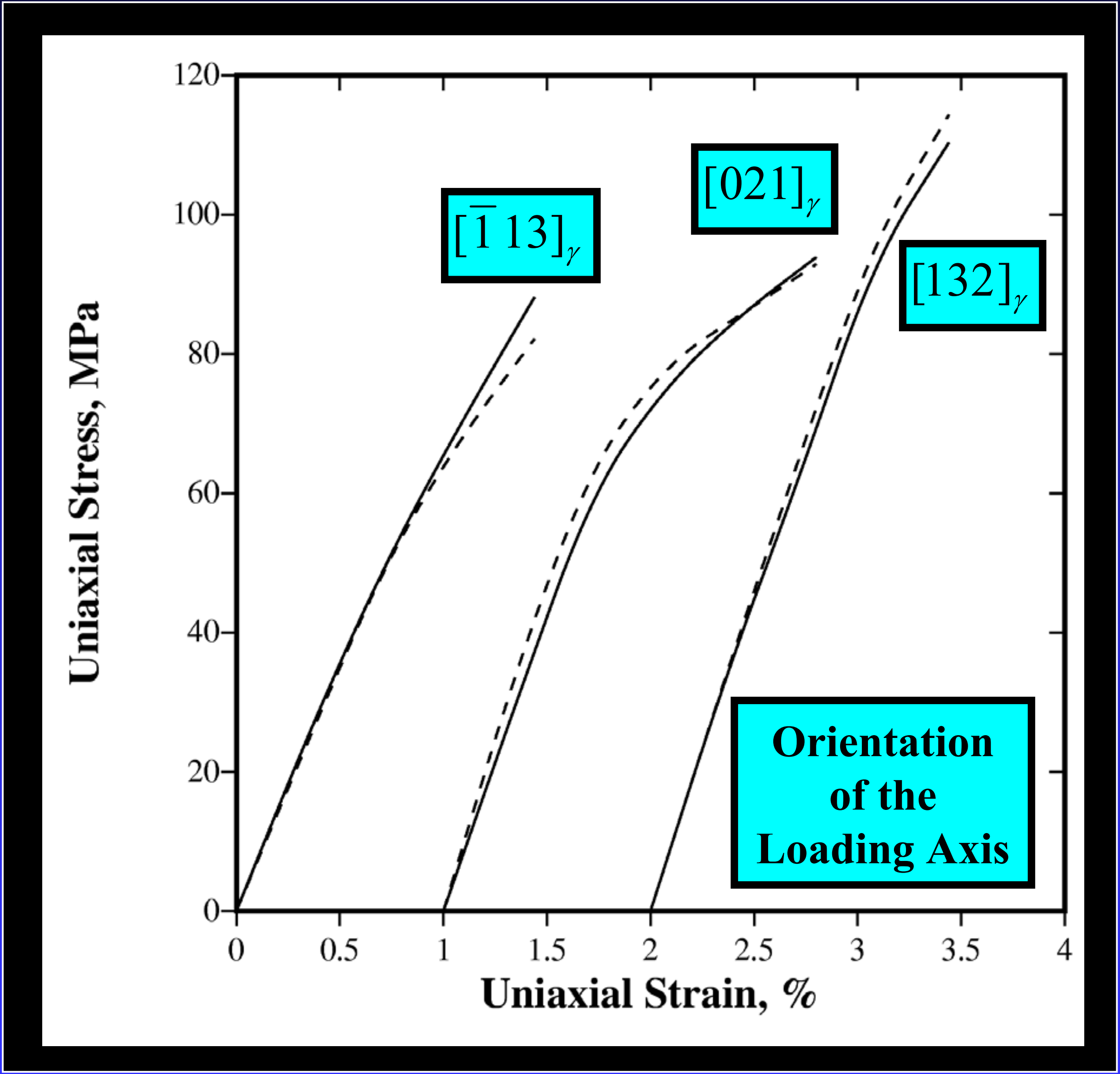

Integration

of the

Material State

Integration of Material State

(a) Compute $F^{p^{-1}}(\tau)$

$$F^{e}(t) = F(t)F^{p^{-1}}(t)$$

$$E^{e}(t) = \frac{1}{2}\left\{F^{e}(t)^{T}F^{e}(t) - I\right\}$$

$$T^{*}(t) = C\left(E^{*}(t)\right)$$

$$\tau^{\alpha}(t) = T^{*}(t)\cdot S_{0}^{\alpha}$$

Integration of Material State, Cont'd.

$$\dot{\gamma}^{\alpha} = \dot{\tilde{\gamma}} \frac{\left|\tau^{\alpha}(t)\right|}{\left|s^{\alpha}(t)\right|}^{\frac{1}{m}} \Delta t$$

$$F^{p^{-1}}(\tau) \cong F^{p^{-1}}(t)\left\{I - \sum_{\alpha} \Delta\gamma^{\alpha}(t) S_0^{\alpha}\right\}$$

(b) Compute Cauchy Stress T(τ)

$$F^{e}(\tau) = F(\tau) F^{p^{-1}}(\tau)$$

$$E^{e}(\tau) = \frac{1}{2}\left\{F^{e}(\tau)^{T} F^{e}(\tau) - I\right\}$$

Integration of Material State, Cont'd.

$$T^*(\tau) = C\left(E^*(\tau)\right)$$

$$T(\tau) = \det(F^*(\tau))^{-1} F^*(\tau) T^*(\tau) F^*(\tau)^T$$

(c) Update Slip Resistances $s^\alpha(\tau)$

$$h^{\alpha\beta}(t) = q^{\alpha\beta}\left|1 - \frac{s^\beta(t)}{s_s}\right|^r sign\left\{1 - \frac{s^\beta(t)}{s_s}\right\}$$

$$s^\alpha(\tau) = s^\alpha(t) + \sum_\beta h^{\alpha\beta}(t)\left|\Delta\gamma^\beta(t)\right|$$

FE Modeling of Deformation and Fracture in Polycrystalline γ-TiAl + α_2-Ti_3Al Single Crystals

Cohesive-Zone Formulation of Colony-Boundary and Lamellar-Interface Potentials

Schematic: γ–TiAl/γ–TiAl (γ1/γ2) bicrystal used for determination of the $(111)_{\gamma1}/(111)_{\gamma2}$ lamellar interfacial potential.

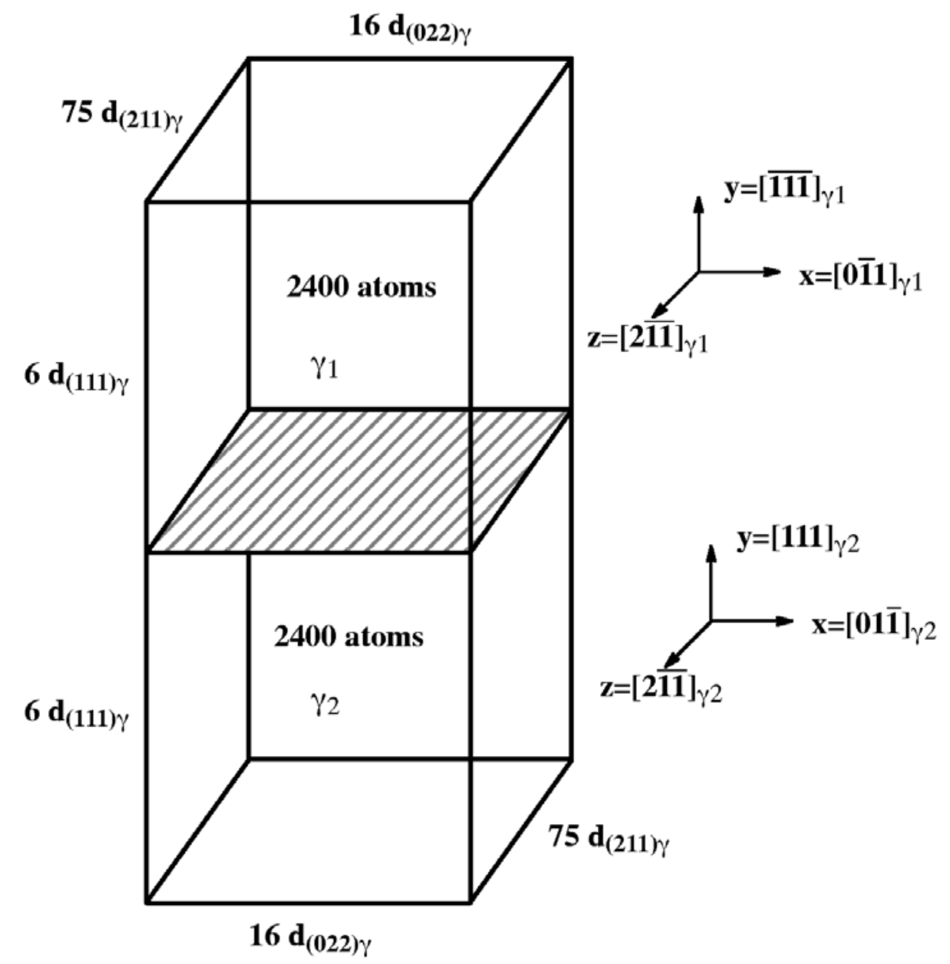

Equilibrium Configuration:

$[\bar{1}\,\bar{1}\,\bar{1}]_{\gamma 1} // [1\,1\,1]_{\gamma 2}$

Lamellar Interface

Projections

(a) The $[0\,1\,\bar{1}]_{\gamma 1} // [0\,\bar{1}\,1]_{\gamma 2}$ plane

(b) The $[\bar{1}\,\bar{1}\,\bar{1}]_{\gamma 1} // [1\,1\,1]_{\gamma 2}$ plane

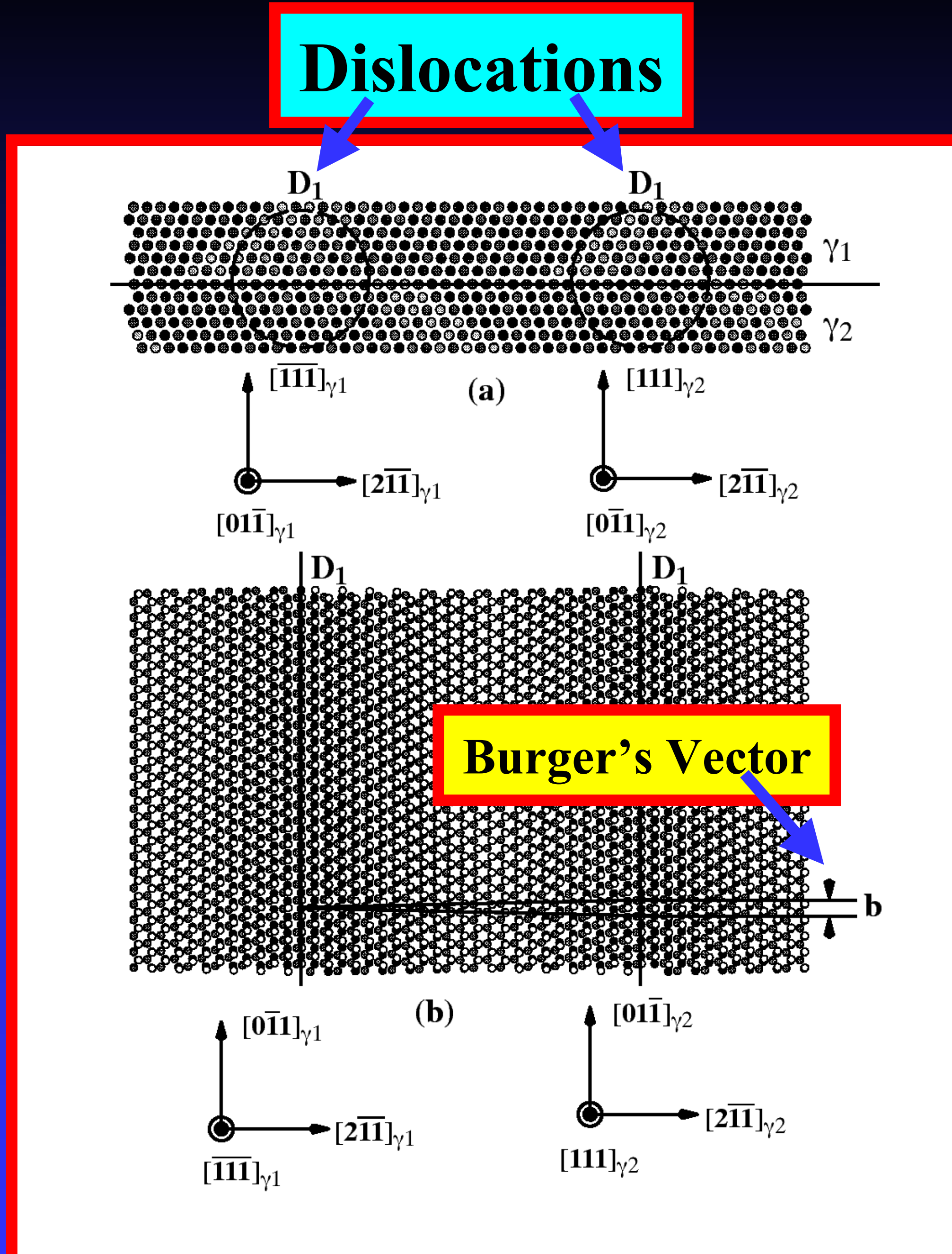

Variation of Interface Potential for $[\bar{1}\,\bar{1}\,\bar{1}]_{\gamma 1} // [1\,1\,1]_{\gamma 2}$ Lamellar Interface

U_n along $[\bar{1}\,\bar{1}\,\bar{1}]_{\gamma 1} // [1\,1\,1]_{\gamma 2}$

U_t along $[0\,1\,\bar{1}]_{\gamma 1} // [0\,\bar{1}\,1]_{\gamma 2}$

U_b along $[2\,\bar{1}\,\bar{1}]_{\gamma 1} // [2\,\bar{1}\,\bar{1}]_{\gamma 2}$

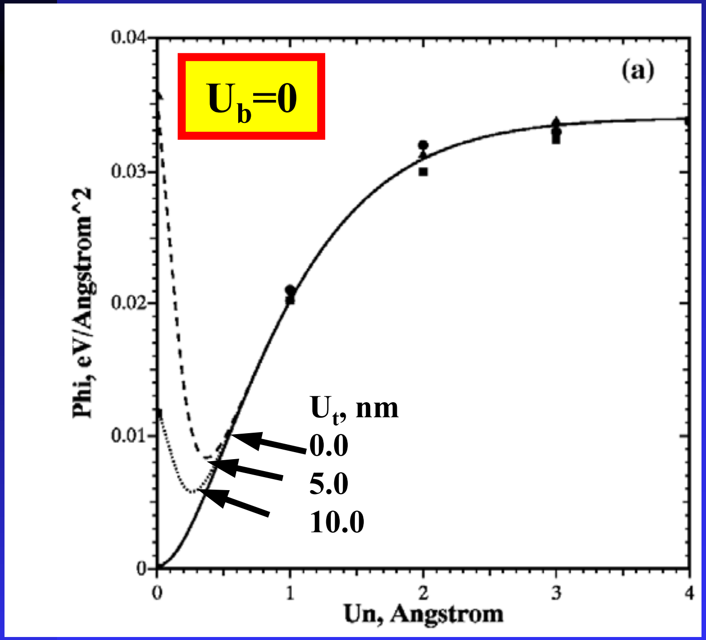

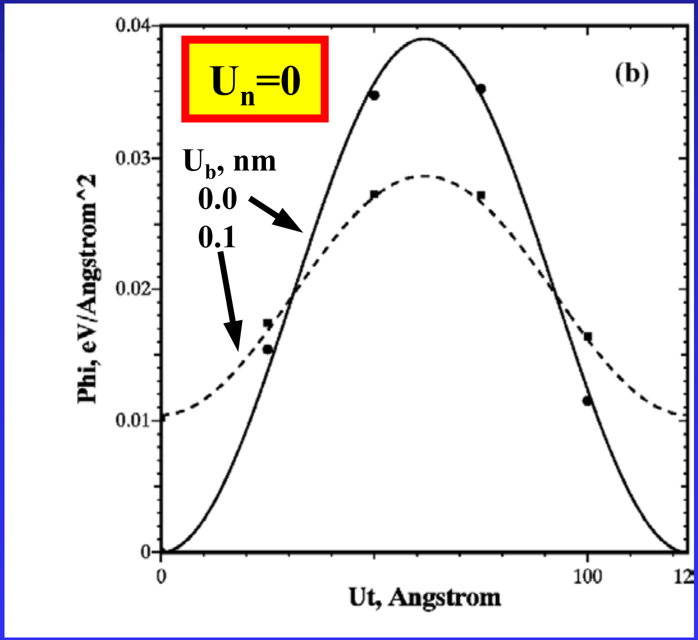

Relationship Between Interface Potential Function Φ and U_n, U_t, and U_b for all γ-TiAl/γ-TiAl Lamellar Interfaces and Colony Boundaries Analyzed

$$\Phi = \sigma_{\max}\delta_n\left[e - \left(\frac{U_n}{\delta_n}+1\right)\exp^{[(U_n/\delta_n)+1]}\right]$$

$$+\frac{1}{2}\alpha_0\left(\frac{6U_n}{\delta_n}+1\right)\exp^{(6U_n/\delta_n)}$$

$$\left\{\alpha_1+\left[\alpha_2\sin\frac{4\pi(U_s-2)}{\lambda_s}+\cos\left(\frac{2\pi U_s}{\lambda_s}+\alpha_3\right)+\alpha_4\right]\left(\alpha_5+\cos\frac{2\pi U_b}{\lambda_b}\right)\right\}$$

Decohesion Potential Parameters for one γ-TiAl/ γ-TiAl Lamellar Interface and one colony boundary

Parameter	Interface Type	
	$(111)_{\gamma 1}/(111)_{\gamma 2}$ Lamellar Boundary	$(001)_{\gamma 1}/(0\bar{1}1)_{\gamma 2}$ Lamellar Boundary
n-Direction	$[\bar{1}\bar{1}\bar{1}]_{\gamma 1}/[111]_{\gamma 2}$	$[001]_{\gamma 1}/[0\bar{1}1]_{\gamma 2}$
t-Direction	$[\bar{1}\bar{1}\bar{1}]_{\gamma 1}/[111]_{\gamma 2}$	$[\bar{1}10]_{\gamma 1}/[\bar{1}\bar{1}\bar{1}]_{\gamma 2}$
b-Direction	$[\bar{1}\bar{1}\bar{1}]_{\gamma 1}/[111]_{\gamma 2}$	$[\bar{1}\bar{1}0]_{\gamma 1}/[2\bar{1}\bar{1}]_{\gamma 2}$
δ_n, nm	0.05	0.05
λ_t, nm	12.35	3.67
λ_b, nm	0.578	1.07

Table Cont'd ↓

Table Cont'd ↑

α_1	-0.039	-0.145
α_2	-1	0.42
α_3	0	-0.31
α_4	0	-3.42
α_5	0	1.17
α_0	0	-5.02
σ_{max}, GPa	2.01	1.21
$\tau_{max,t}$, GPa	0.160	12.7
$\tau_{max,b}$, GPa	1.65	0.73
$\Phi(U_n \rightarrow \infty)$, J/m^2	0.561	0.374

Interface Elements

Reference Configuration

Nodes: 1=4 & 2=3

Internal Nodes

Internal Nodes

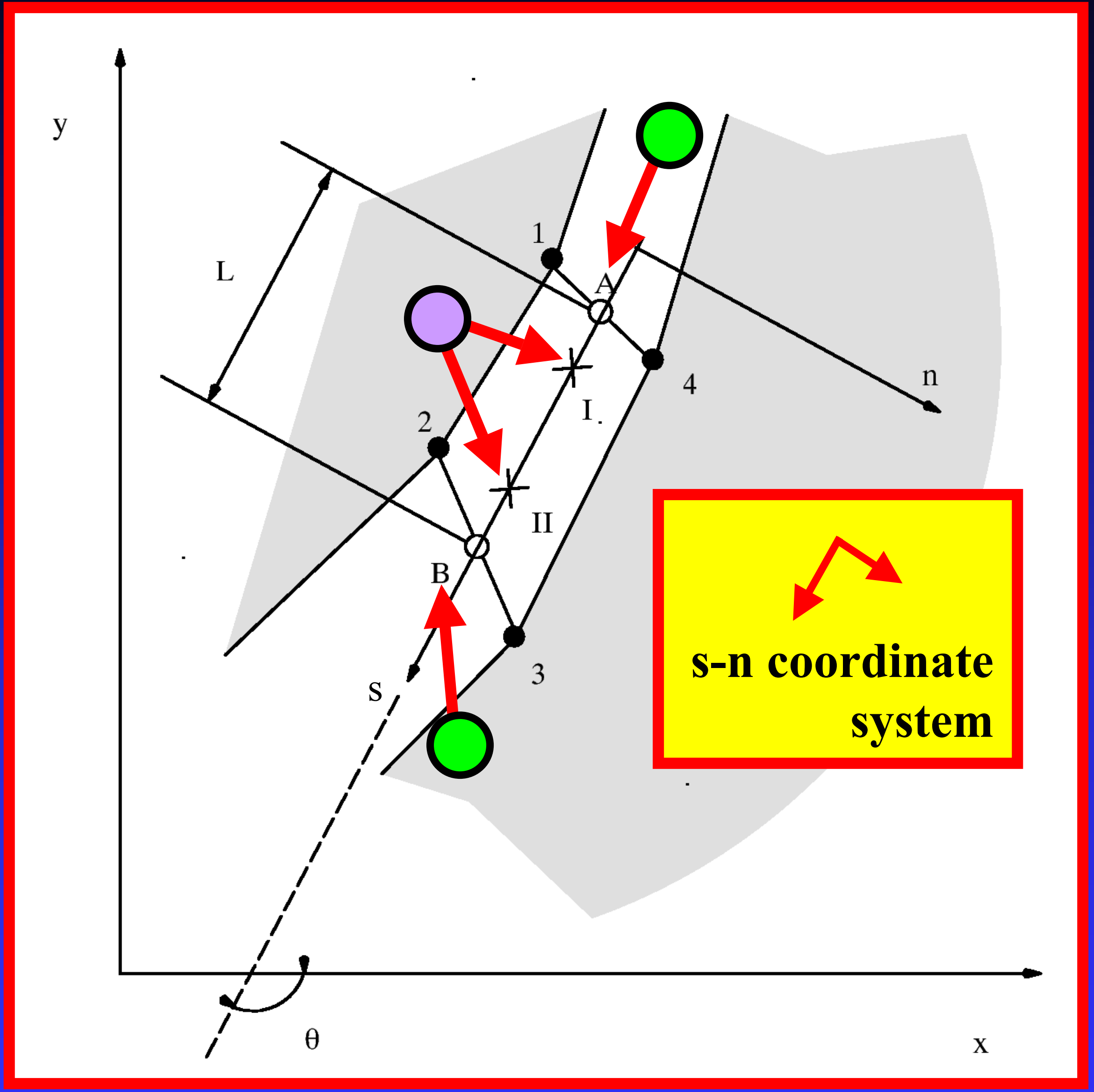

Interface Element Formulation

Interface Displacements:

Displacements at nodes A&B mapped to those at nodes 1, 2, 3 and 4

$$U_n^A = (U_y^4 - U_y^1)\cos\theta - (U_x^4 - U_x^1)\sin\theta$$

$$U_s^A = (U_y^4 - U_y^1)\sin\theta - (U_x^4 - U_x^1)\cos\theta$$

$$U_n^B = (U_y^3 - U_y^2)\cos\theta - (U_x^3 - U_x^2)\sin\theta$$

$$U_n^A = (U_y^4 - U_y^1)\cos\theta - (U_x^4 - U_x^1)\sin\theta$$

Interface Element Formulation Cont'd:

Normal and Tangential Components of Interface Displacements:

$$U_s(\eta) = N_A(\eta)U_s^A + N_B(\eta)U_s^B$$

$$U_n(\eta) = N_A(\eta)U_n^A + N_B(\eta)U_n^B$$

Virtual Work Equation:

$$\int_{-1}^{1} \delta\Phi(\eta) L \pi r(\eta) d\eta = \sum_{I=n.s} \sum_{N=A.B} F_I^N \delta U_I^N$$

Interface Element Formulation Cont'd:

Perturbation of Interface Potential:

$$\partial\Phi = \frac{\partial\Phi[U_s(\eta), U_n(\eta)]}{\partial U_n}\left[N_A(\eta)\delta U_n^A + N_B(\eta)\delta U_n^B\right] + \frac{\partial\Phi[U_s(\eta), U_n(\eta)]}{\partial U_s}\left[N_A(\eta)\delta U_s^A + N_B(\eta)\delta U_s^B\right]$$

Force Components at Nodes A and B:

$$F_I^N = \int_{-1}^{1} \frac{\partial\Phi[U_s(\eta), U_n(\eta)]}{\partial U_I} N_N(\eta) L \pi r(\eta) d\eta$$

Interface Element Formulation Cont'd:

Residual Nodal Forces in Global Coordinate System:

$$R_x^1 = -R_x^4 = F_s^A \cos\theta - F_n^A \sin\theta$$
$$R_y^1 = -R_y^4 = F_s^A \sin\theta - F_n^A \cos\theta$$
$$R_x^2 = -R_x^3 = F_s^B \cos\theta - F_n^B \sin\theta$$
$$R_y^2 = -R_y^3 = F_s^B \sin\theta - F_n^B \cos\theta$$

Components of the Element jacobian:

$$\frac{\partial R_j^i}{\partial U_I^k} = \sum_{I=n.s}\sum_{N=A.B}\sum_{j=n.s}\sum_{M=A.B} \frac{\partial R_j^i}{\partial F_I^N}\frac{\partial F_I^N}{\partial U_J^M}\frac{\partial U_J^M}{\partial U_I^k}$$

Finite Element

Formulation and

Results

Polycrystalline Aggregate

Finite Element Mesh

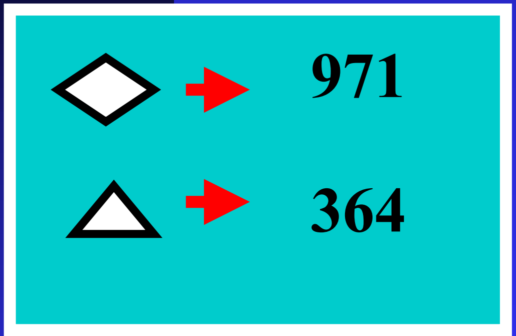

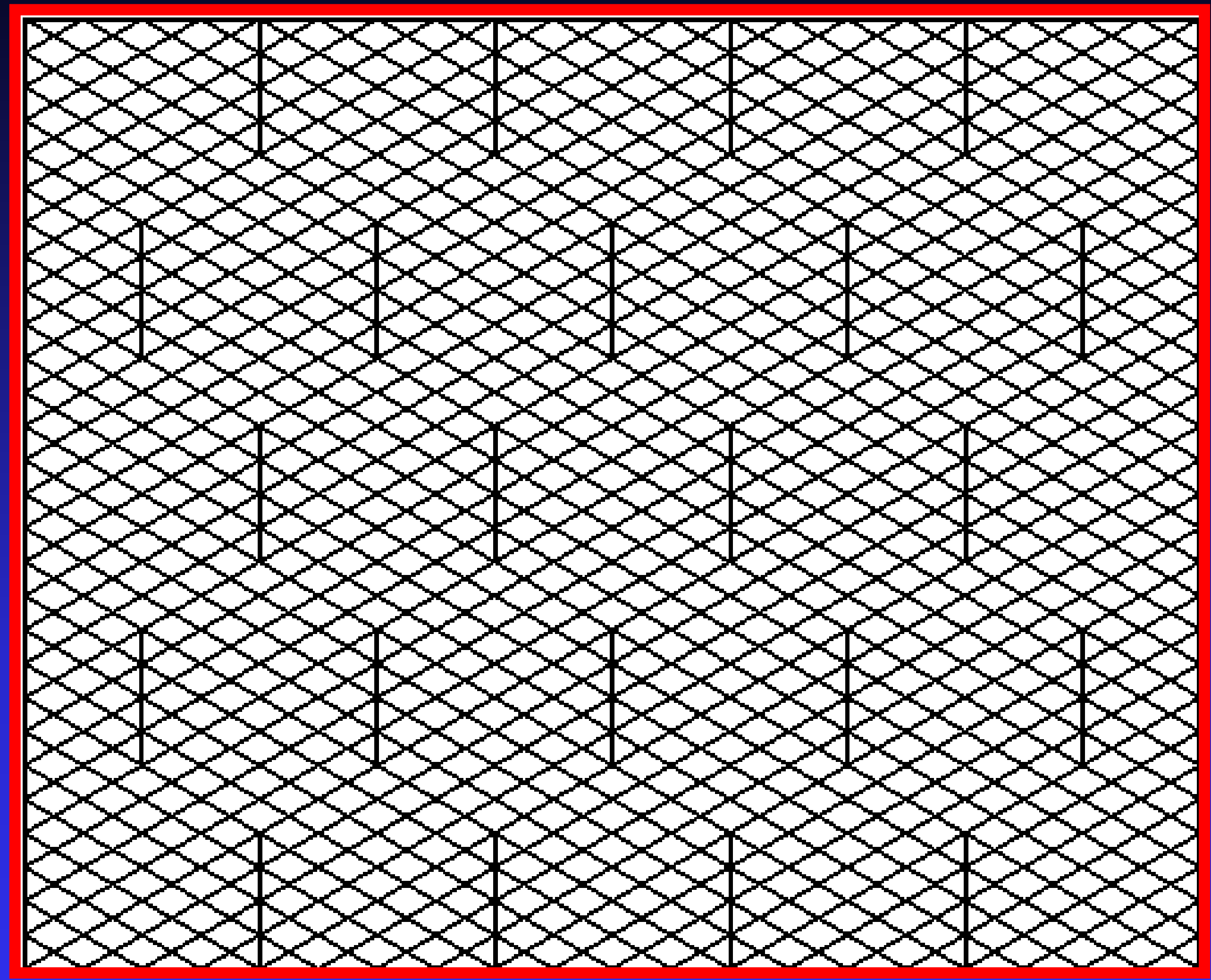

Polycrystalline Aggregate of 27 Lamellar Colonies

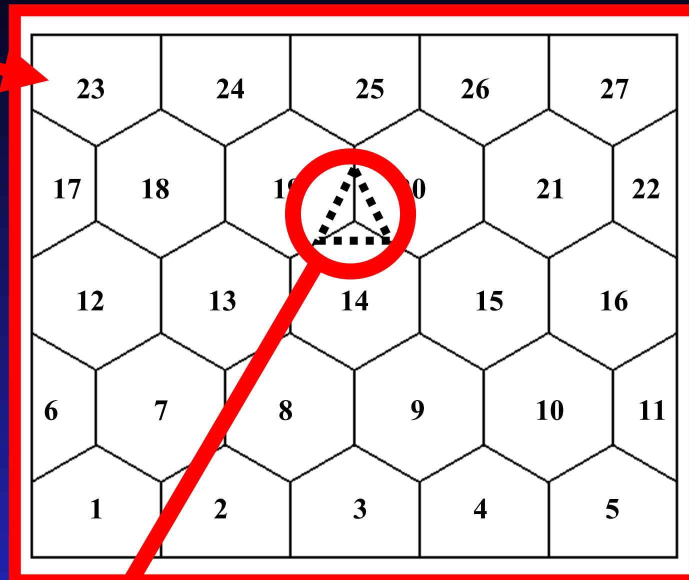

Reference Configuration With 3 Lamellar Colonies Each Having 2 Lamellar Boundaries

Finite Element Mesh

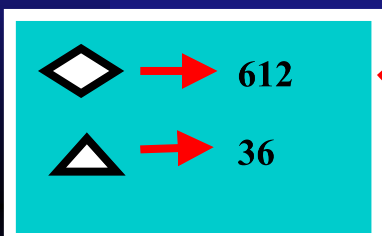

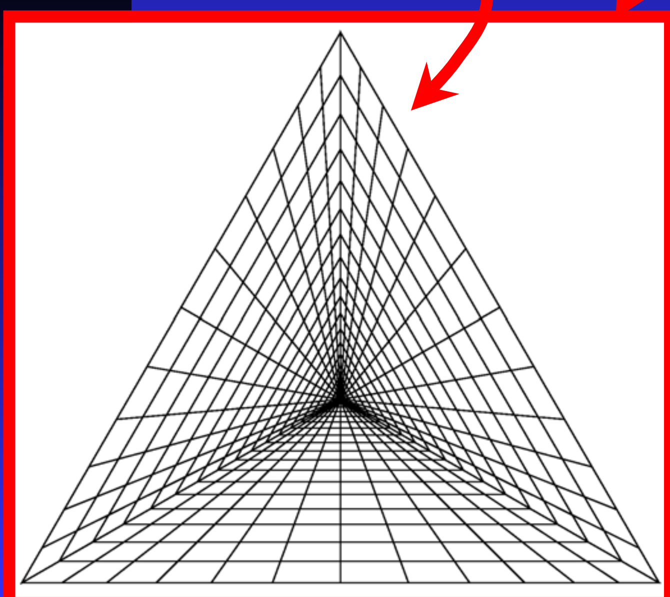

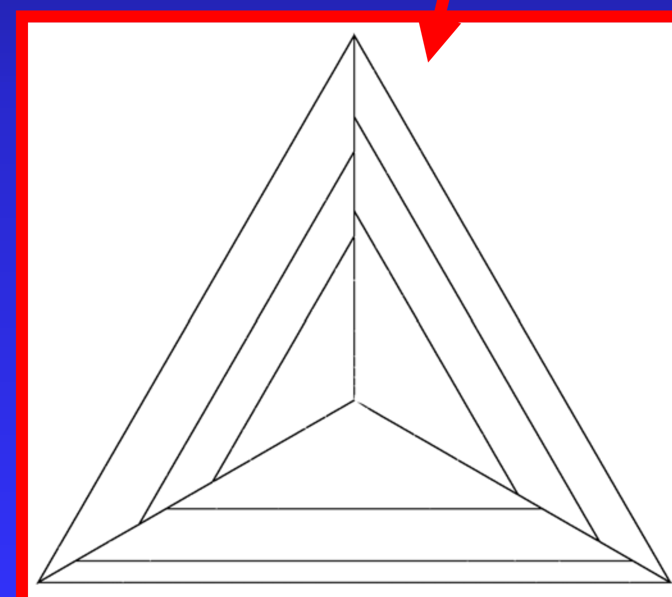

Results

Equivalent Plastic Strain

ε=0.015

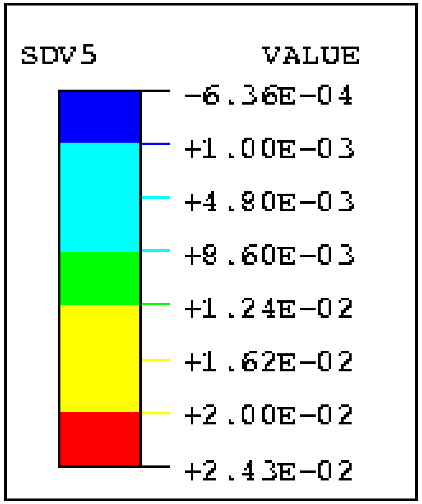

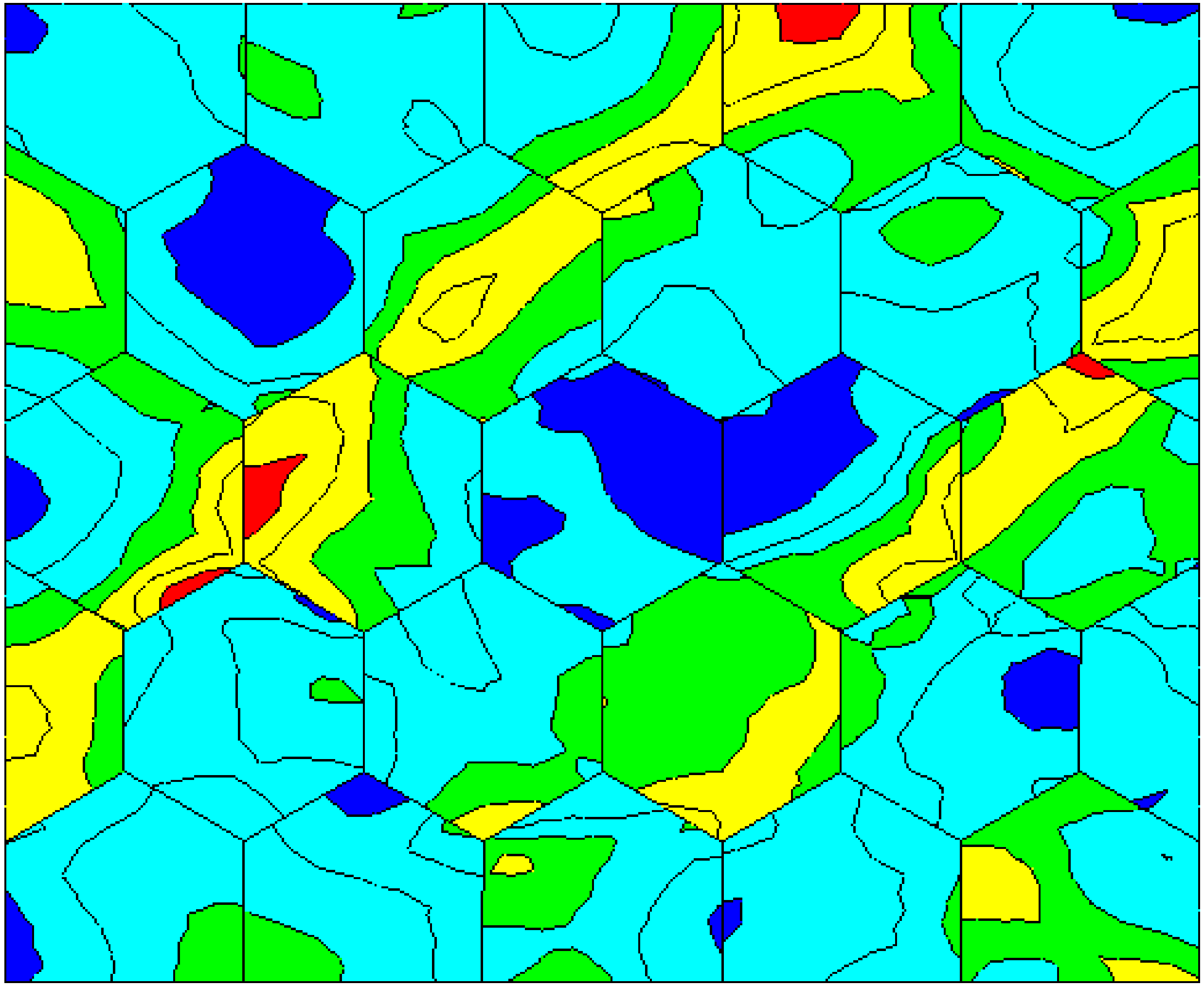

Results Contd.

Lattice Rotation

ε=0.015

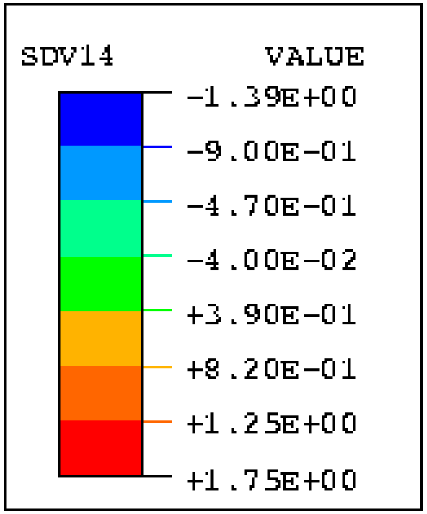

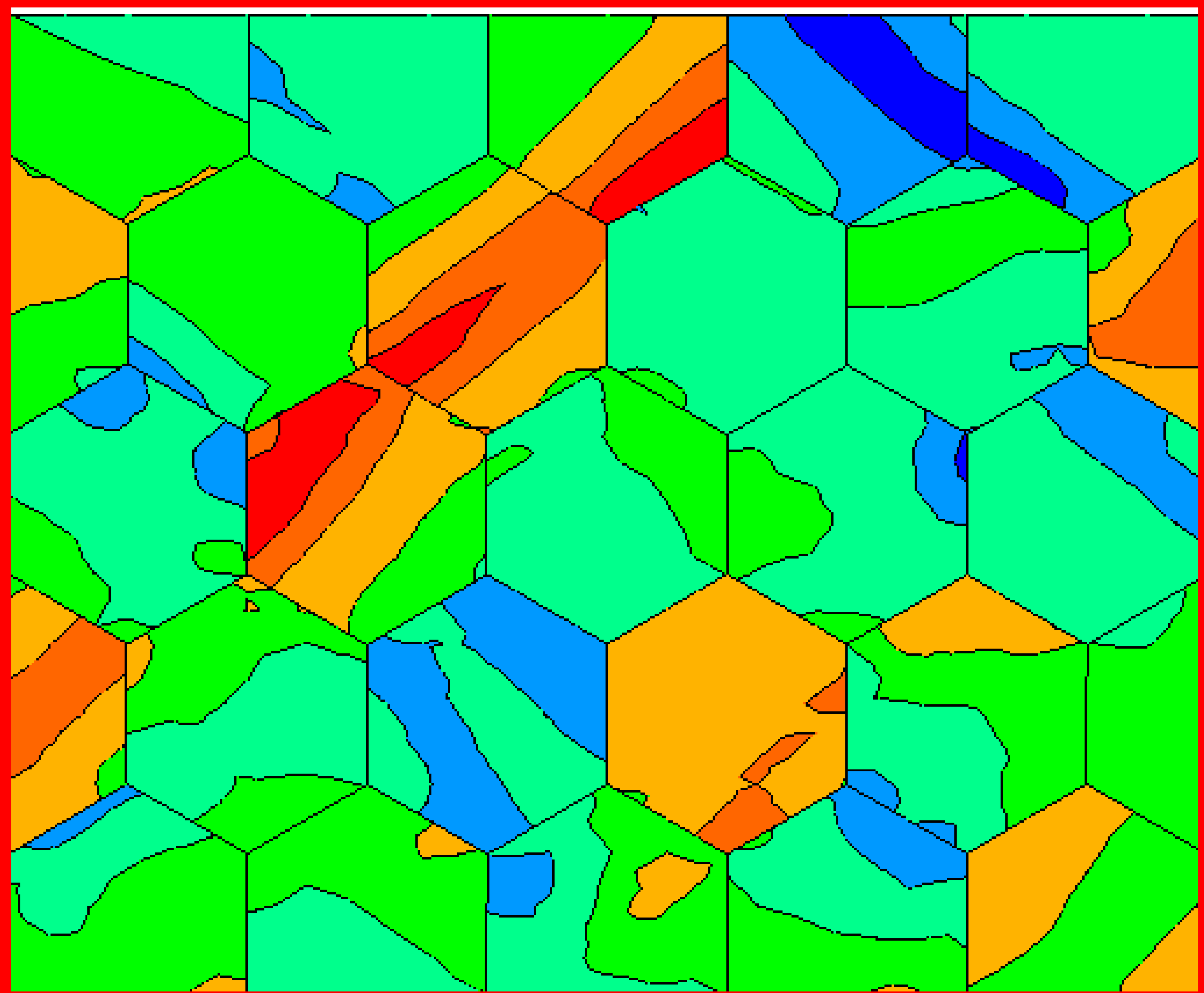

Results Contd.

Hydrostatic Stress

$\varepsilon=0.015$

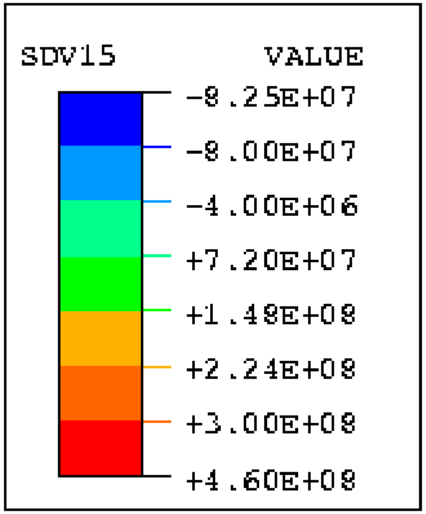

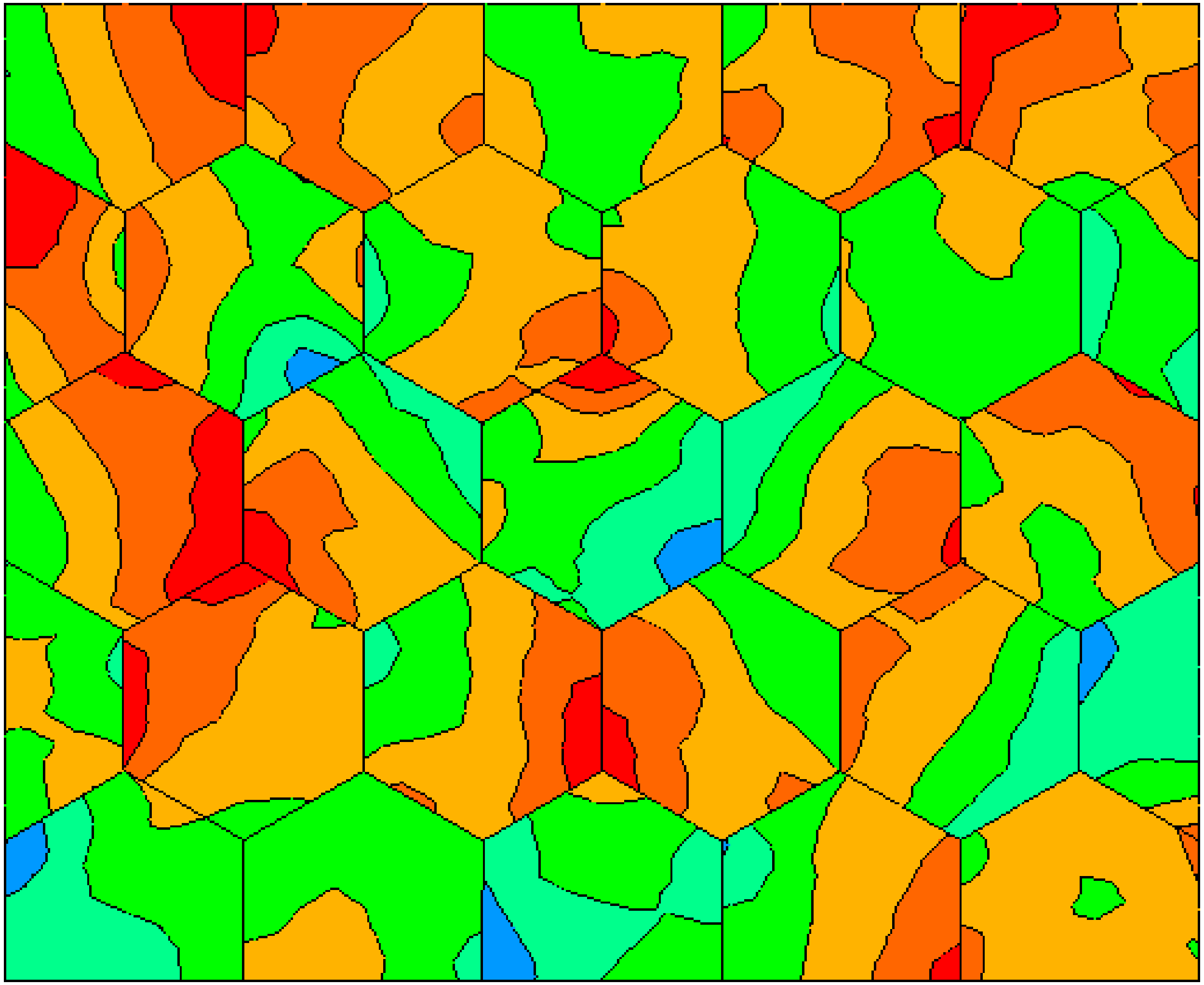

Results Contd.

Equivalent Stress

ε=0.015

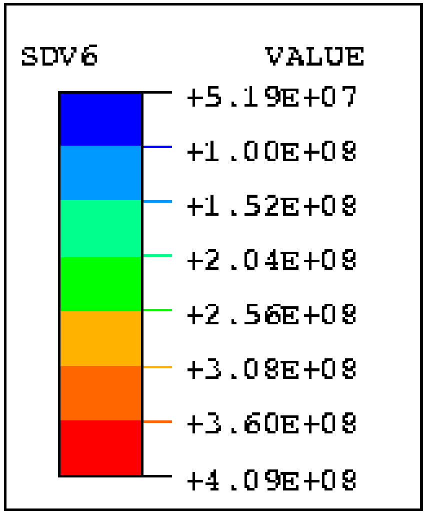

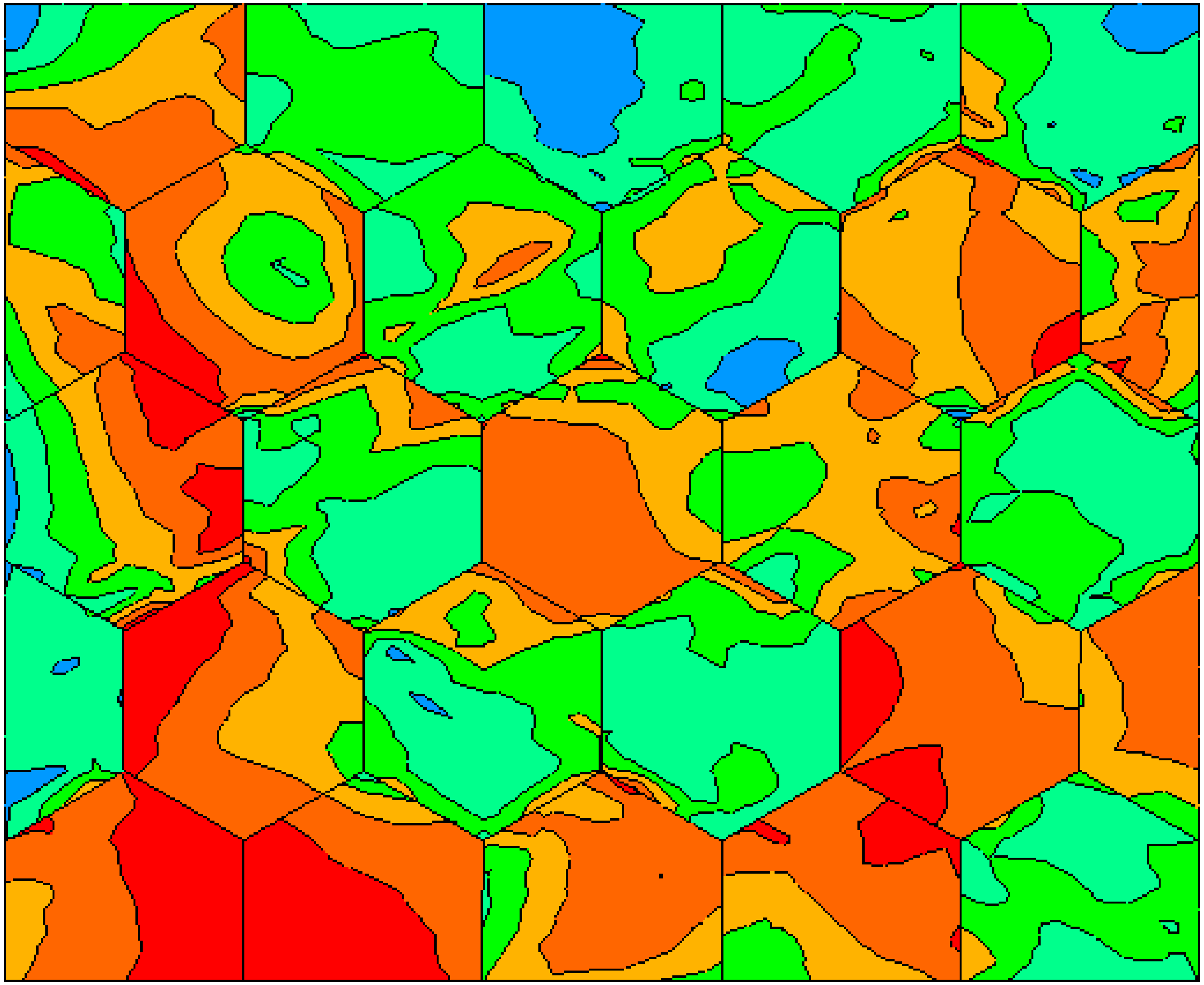

Results Contd.

Equivalent Plastic Strain

ε=0.03

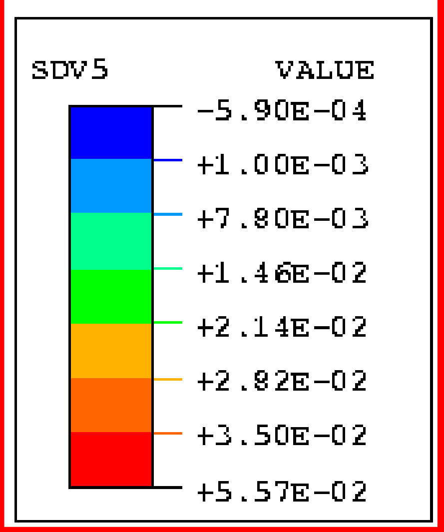

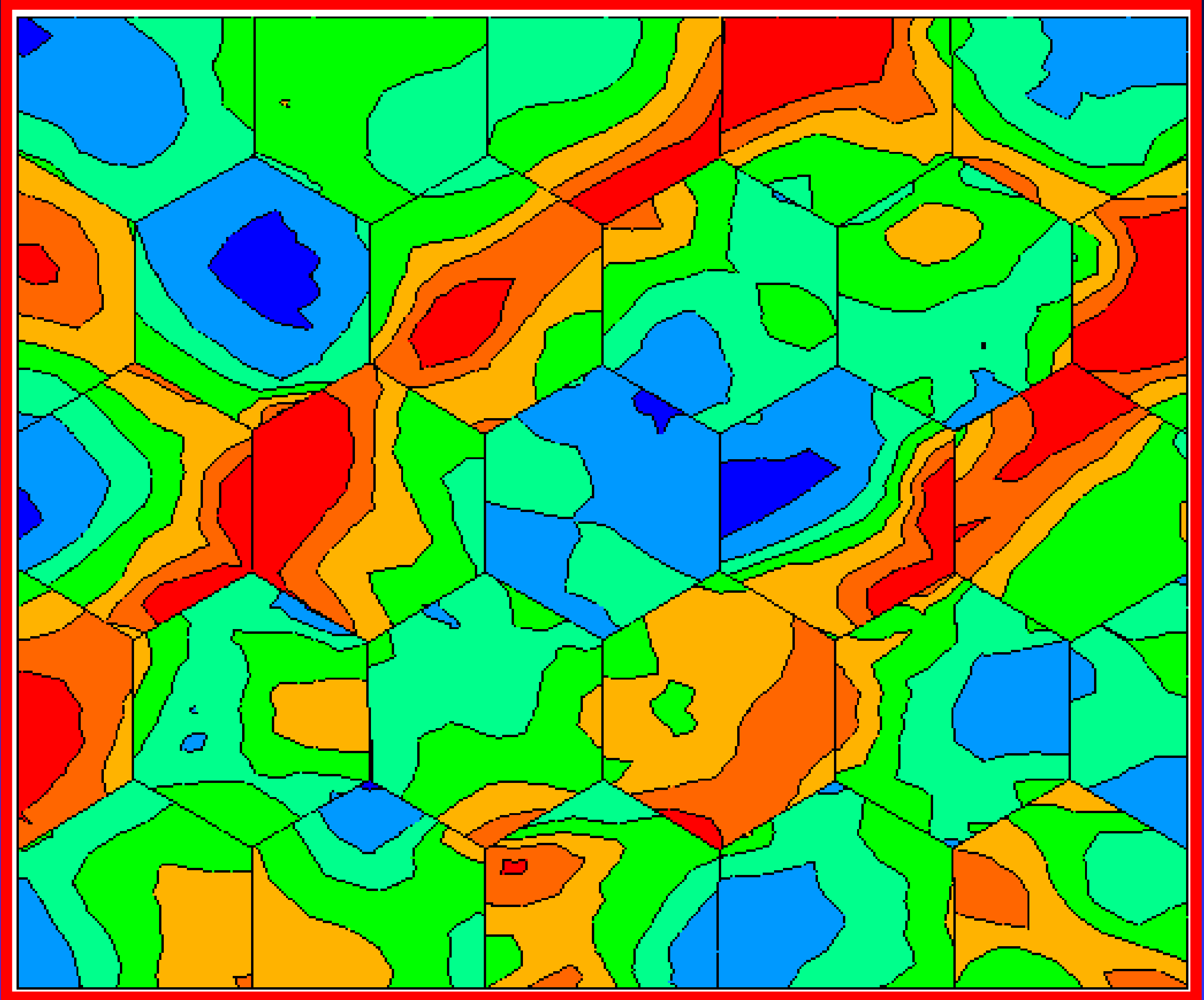

Results Contd.

Lattice Rotation

ε=0.03

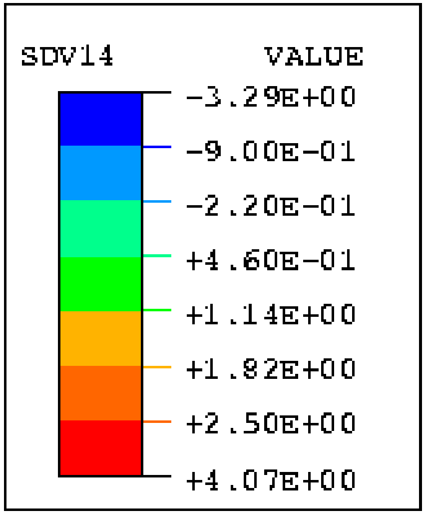

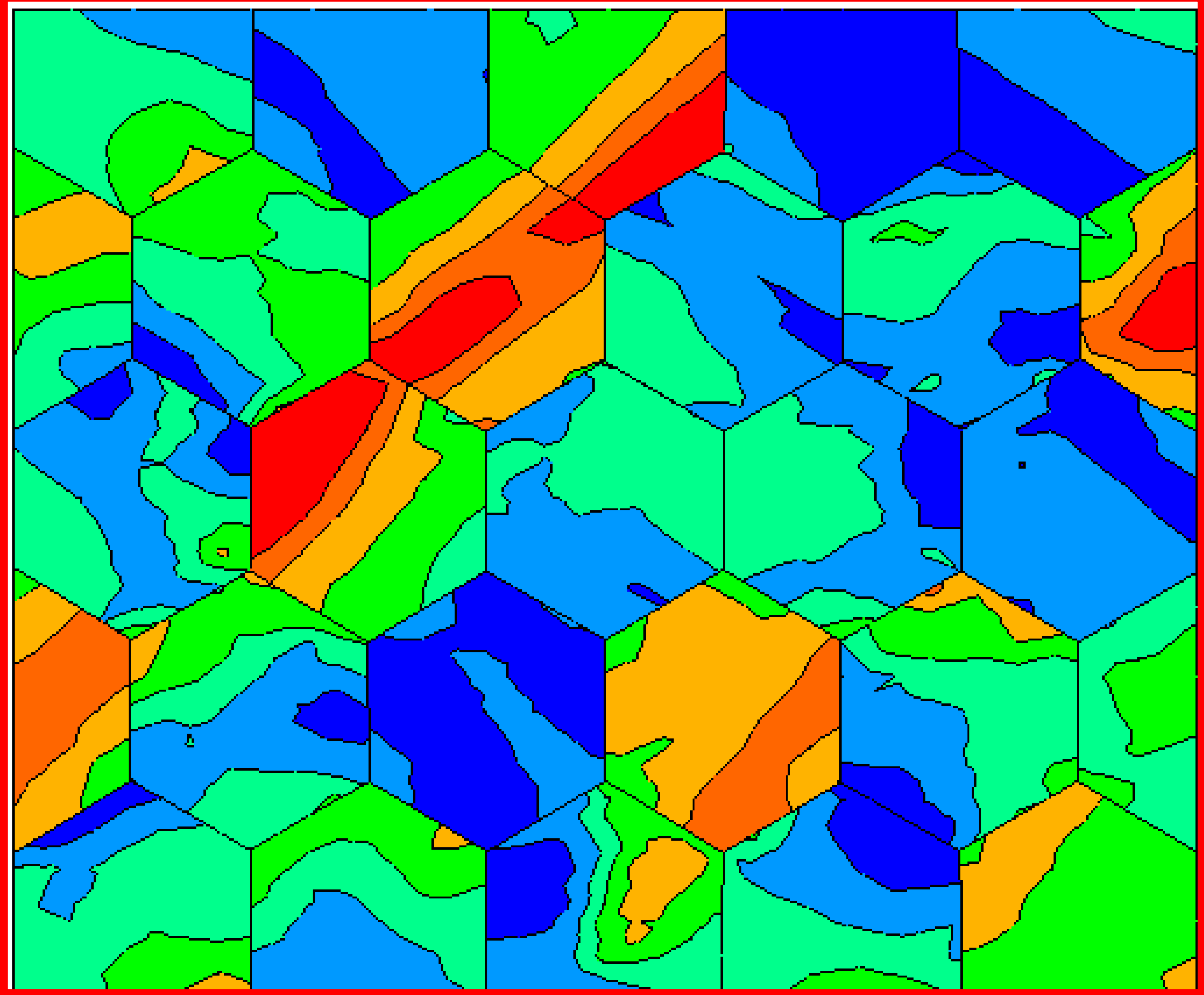

Results Contd.

Hydrostatic Stress

ε=0.03

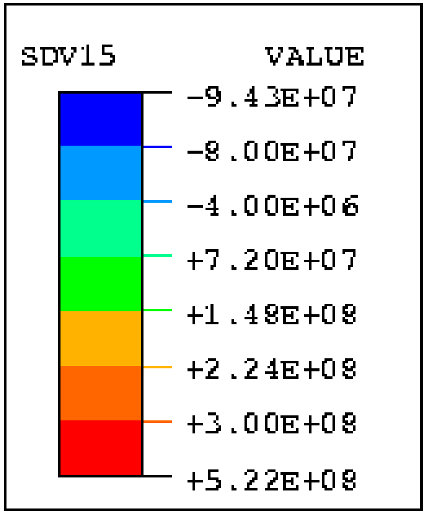

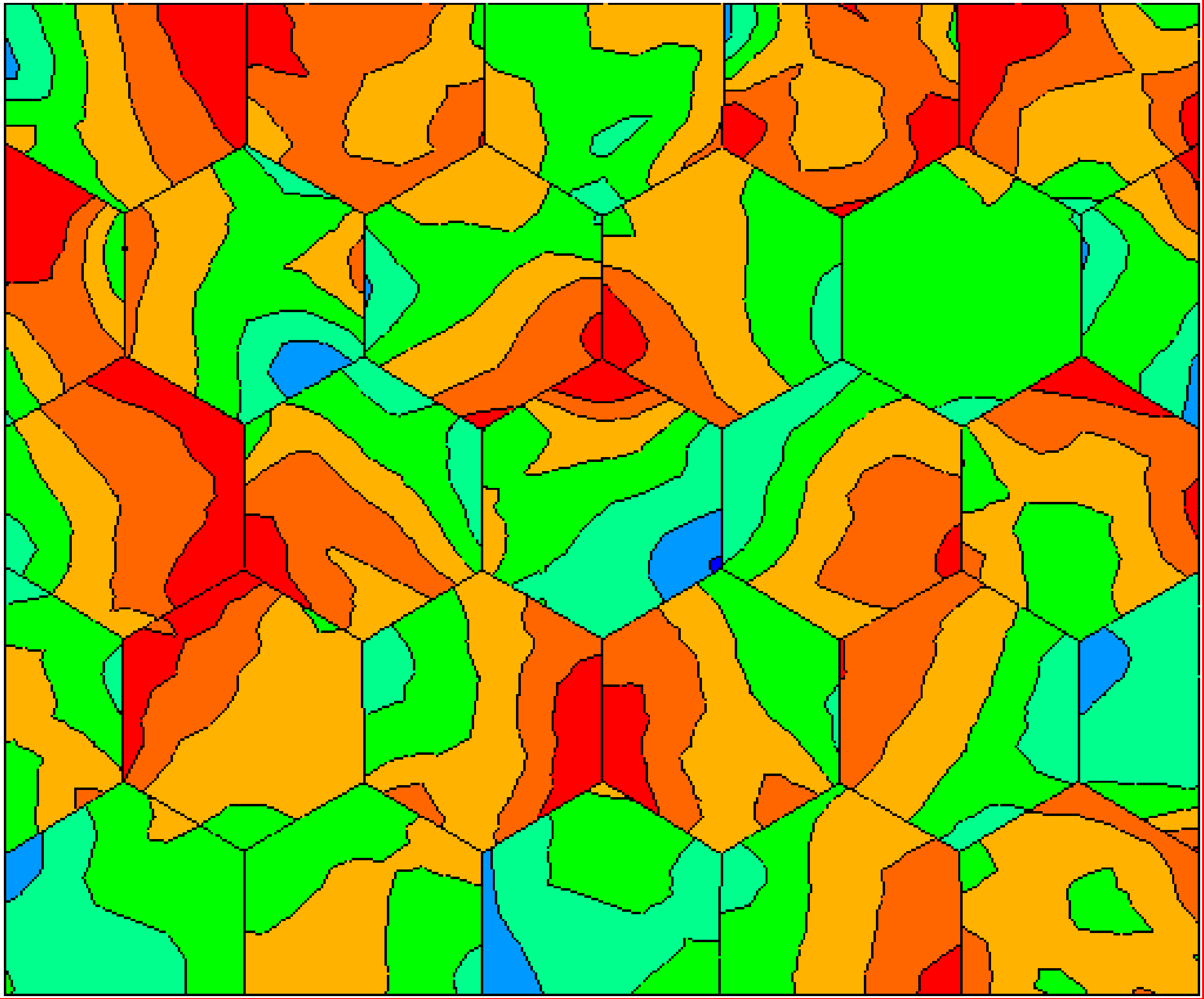

Results Contd.

Equivalent Stress

ε=0.03

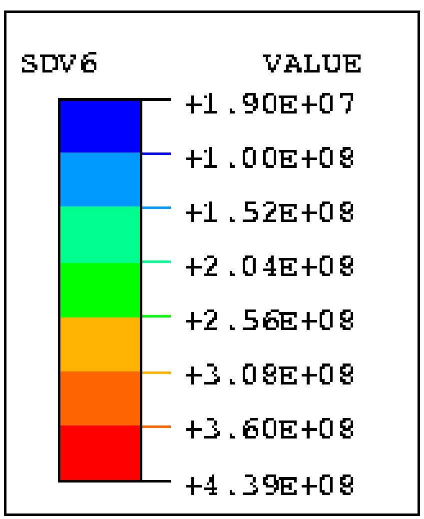

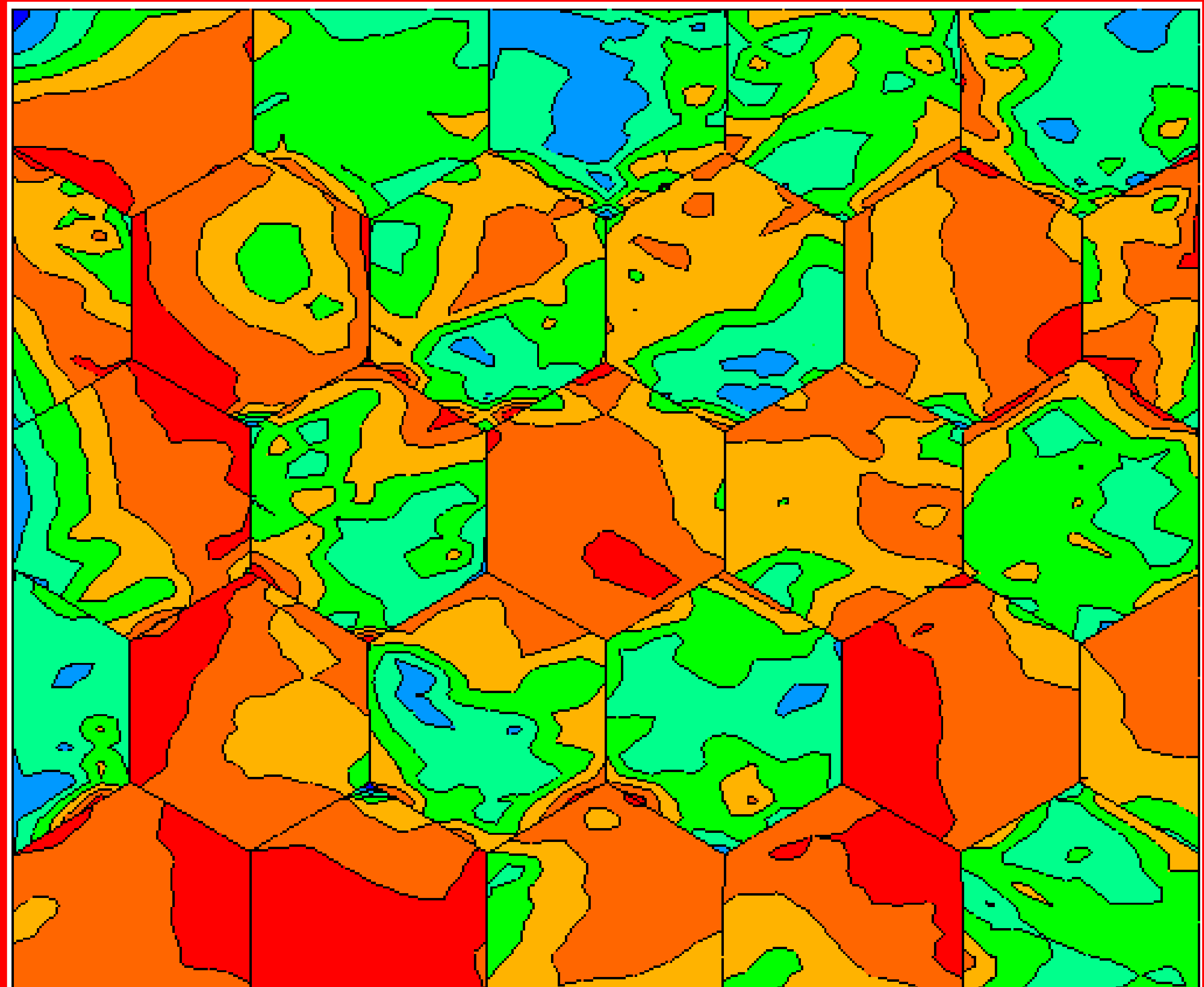

Results Contd.

Hydrostatic Stress

ε=0.03

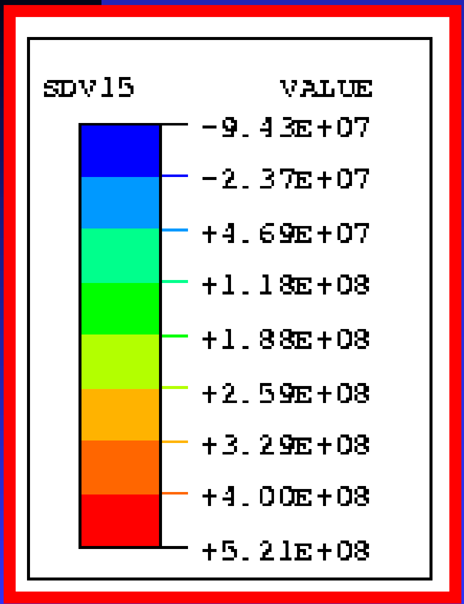

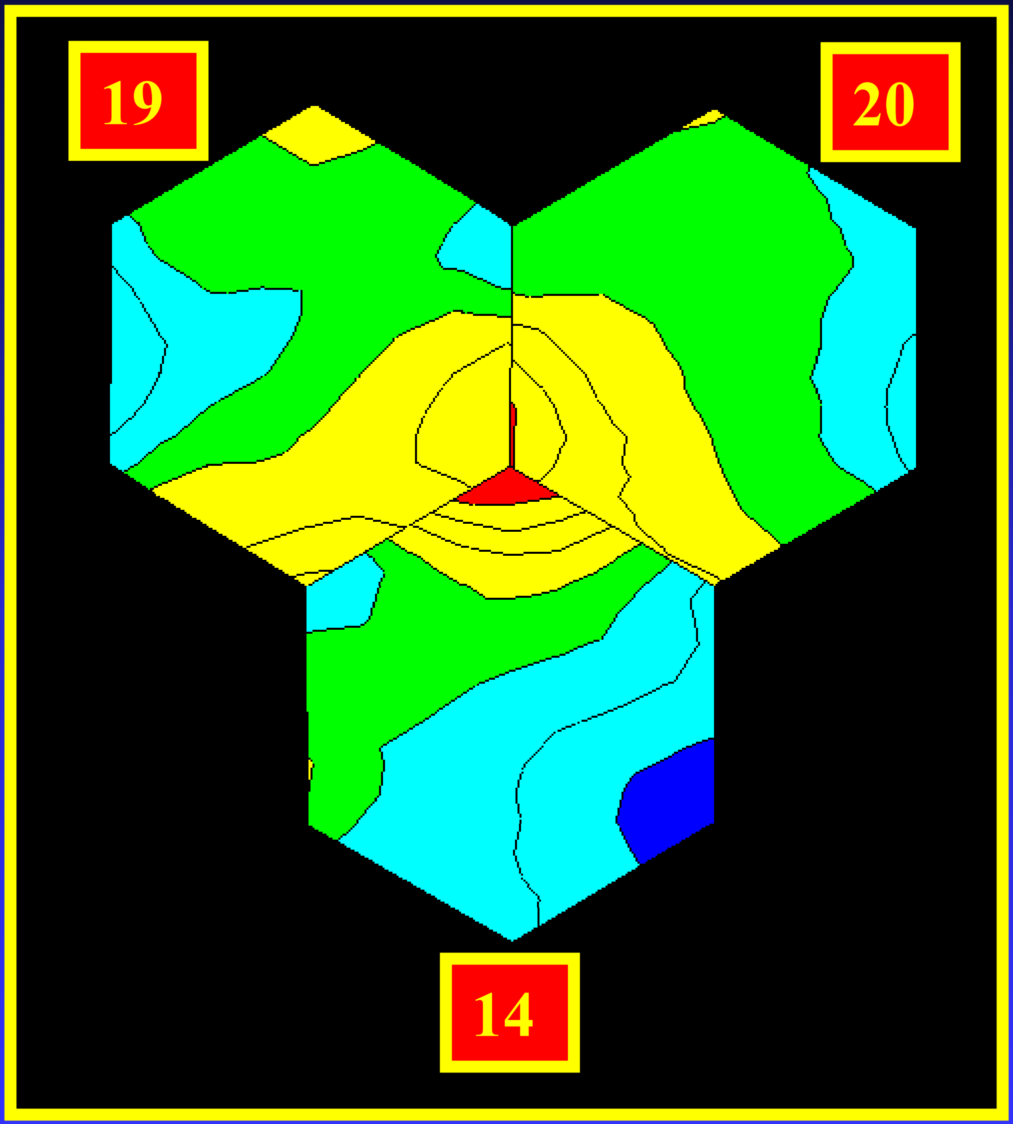

Results Contd.

Hydrostatic Stress

ε=0.0319

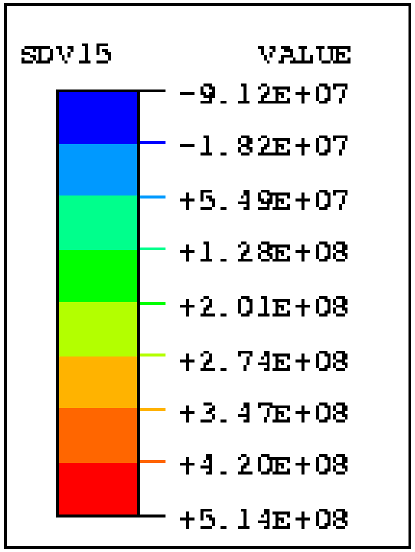

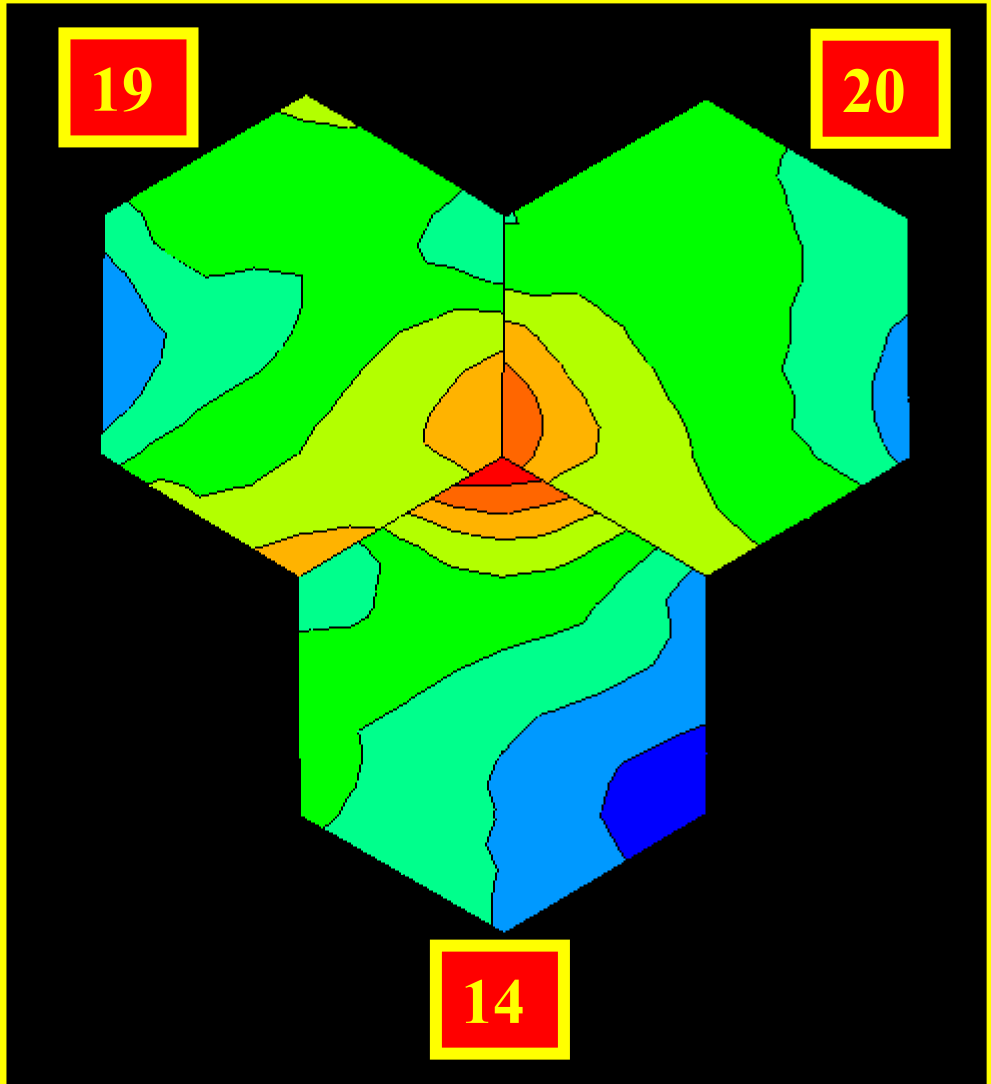

Results Contd.

Around 3-Colony Junction

$\varepsilon=0.025$

No Lamellar Interfaces

Equivalent Plastic Strain

Hydrostatic Stress

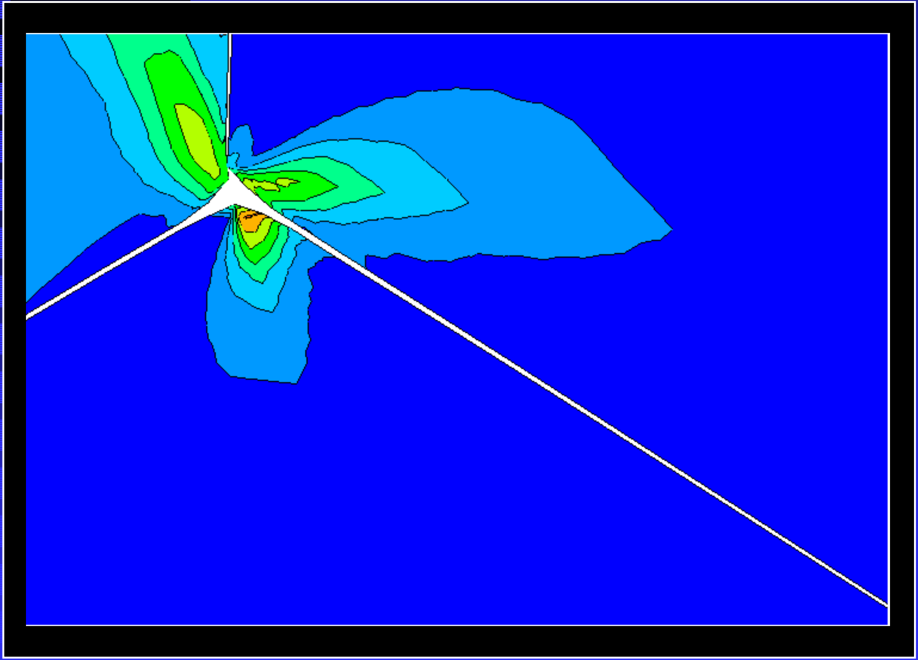

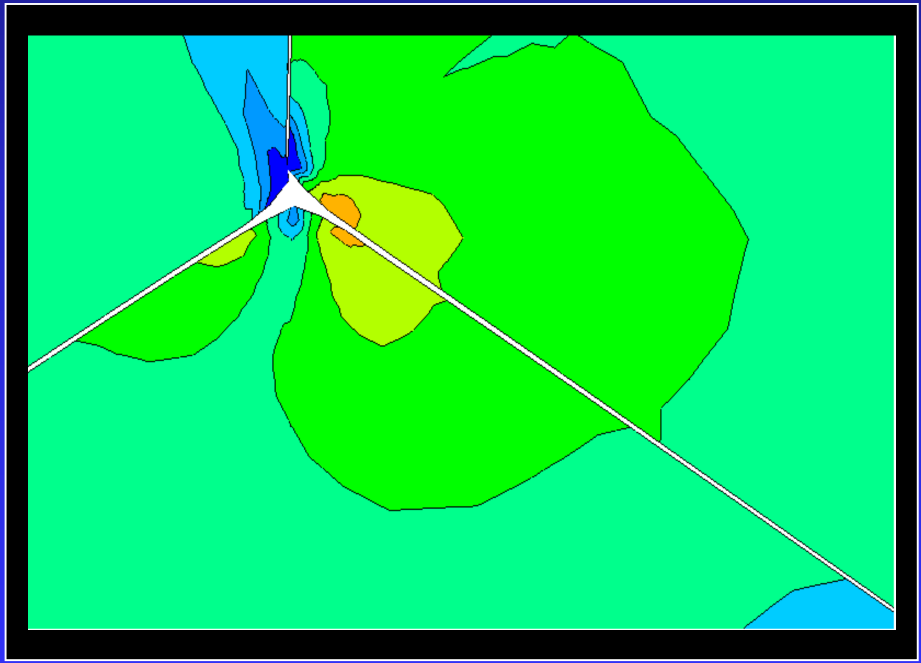

Results Contd.

Around 3-Colony Junction

$\varepsilon=0.030$

No Lamellar Interfaces

Equivalent Plastic Strain

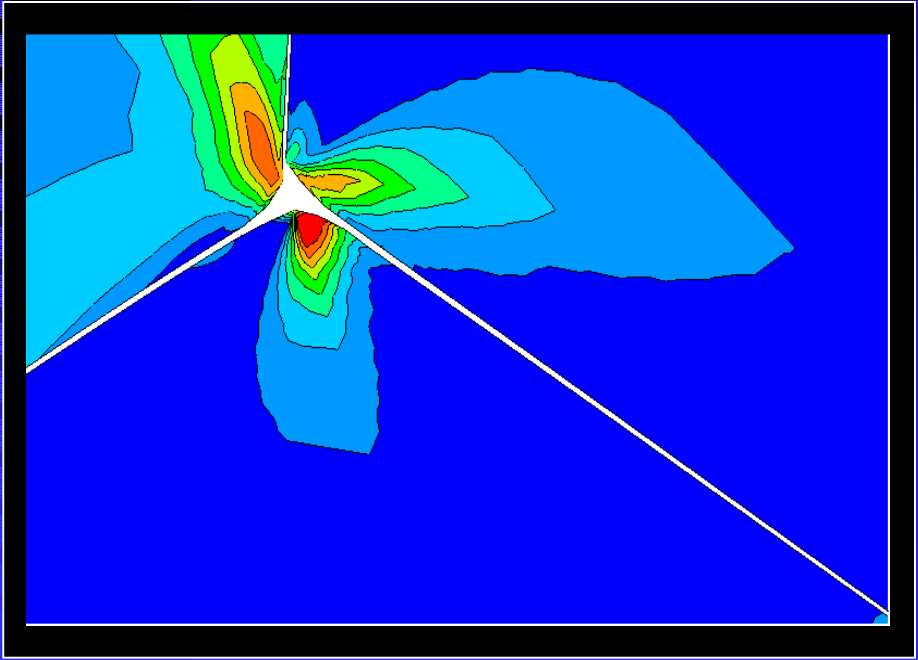

Hydrostatic Stress

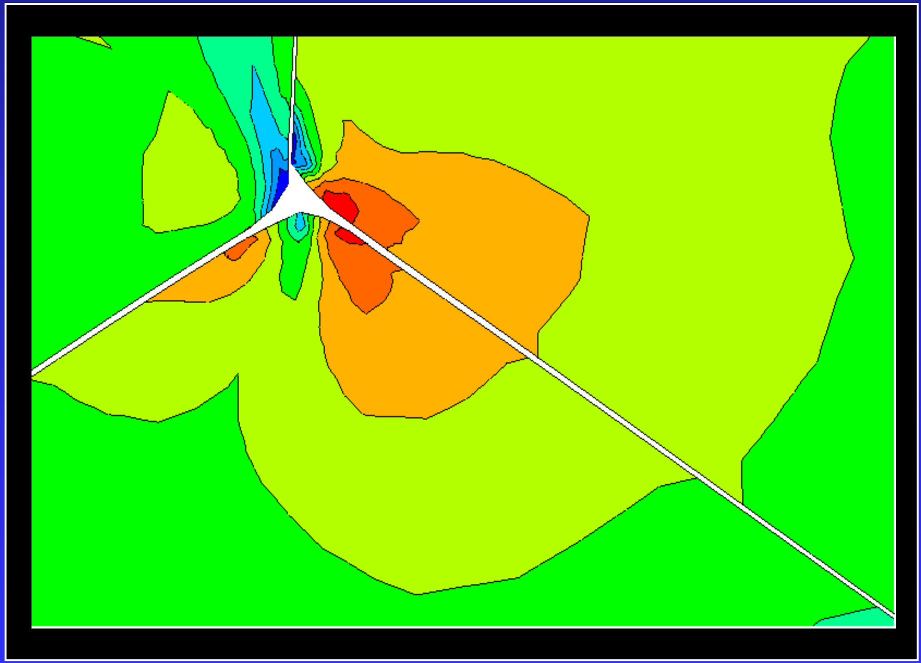

Results Contd.

Around 3-Colony Junction

ε=0.0319

No Lamellar Interfaces

Equivalent Plastic Strain

Hydrostatic Stress

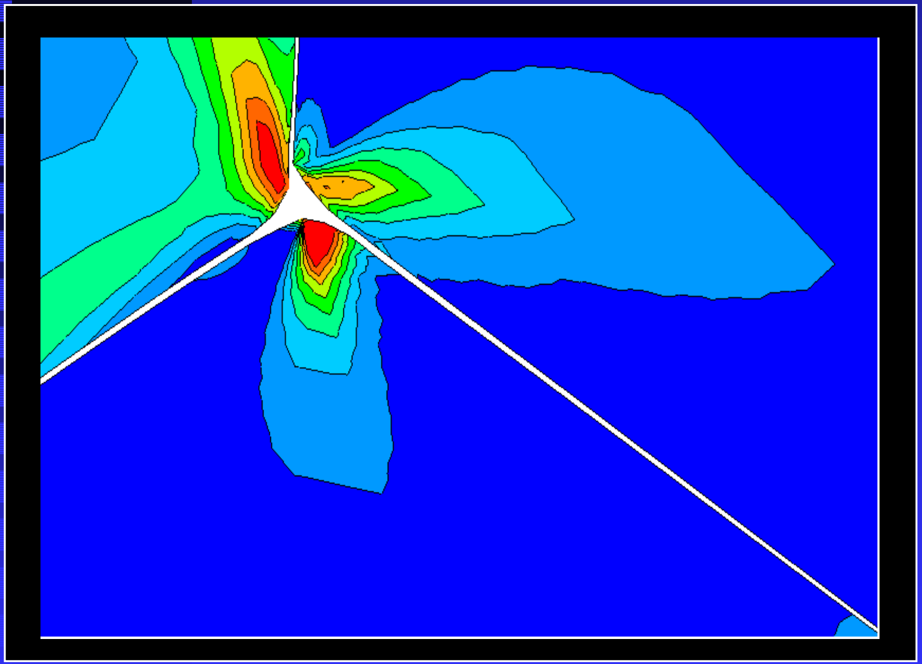

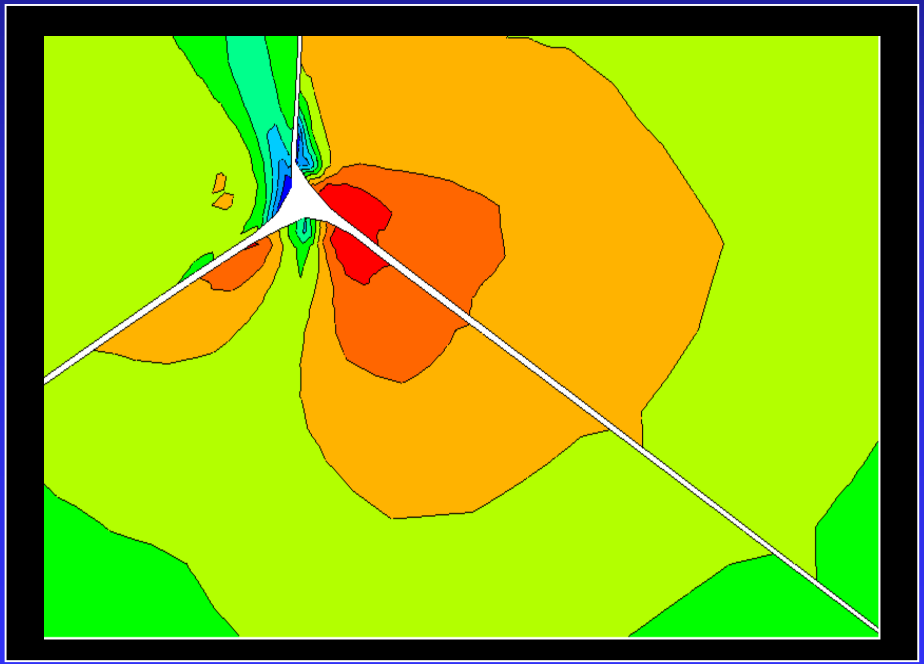

Results Contd.

Around 3-Colony Junction

$\varepsilon = 0.0250$

With Lamellar Interfaces

Equivalent Plastic Strain

Hydrostatic Stress

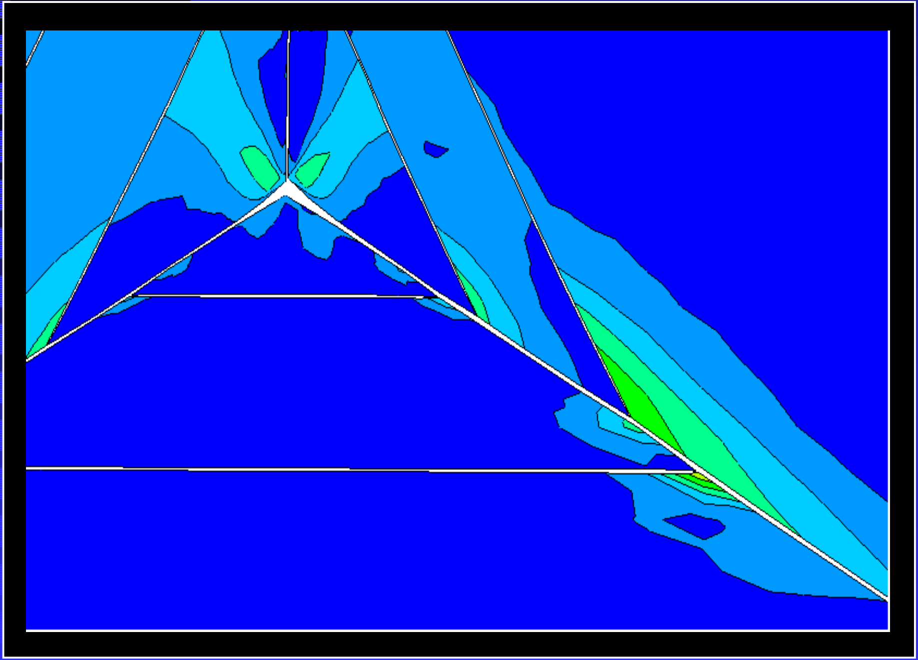

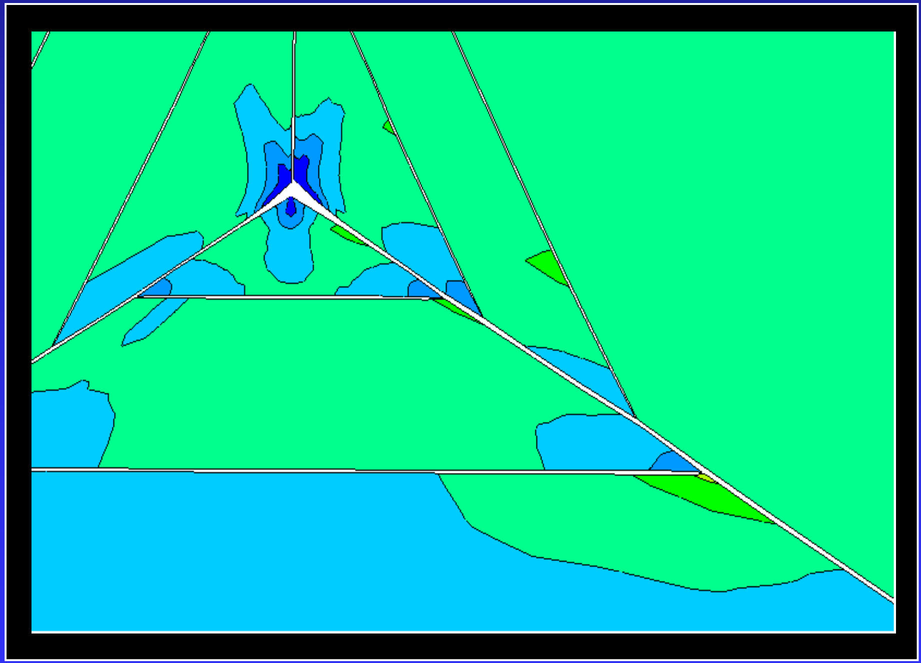

Results Contd.

Around 3-Colony Junction

ε=0.030

With Lamellar Interfaces

Equivalent Plastic Strain

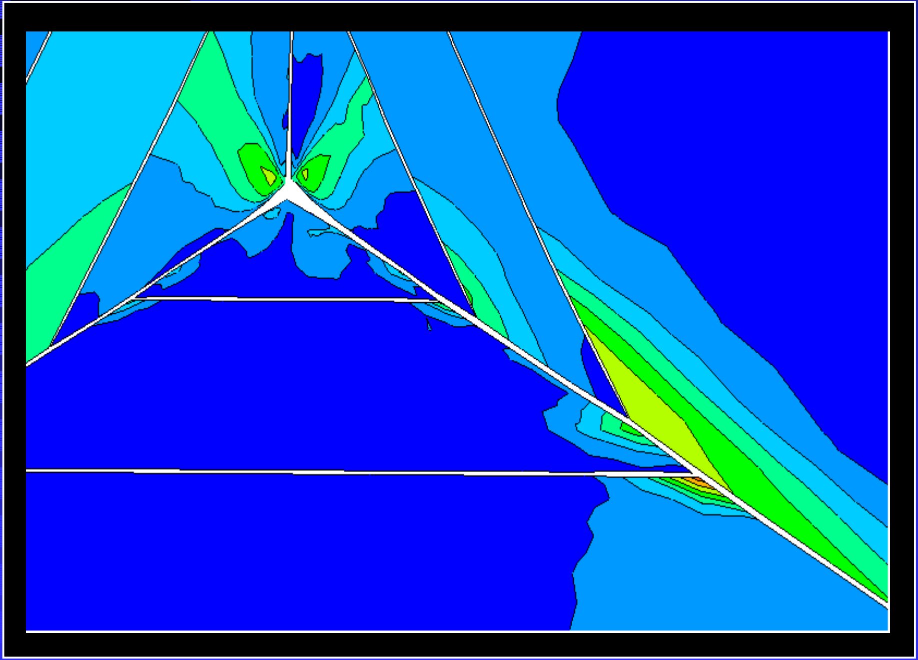

Hydrostatic Stress

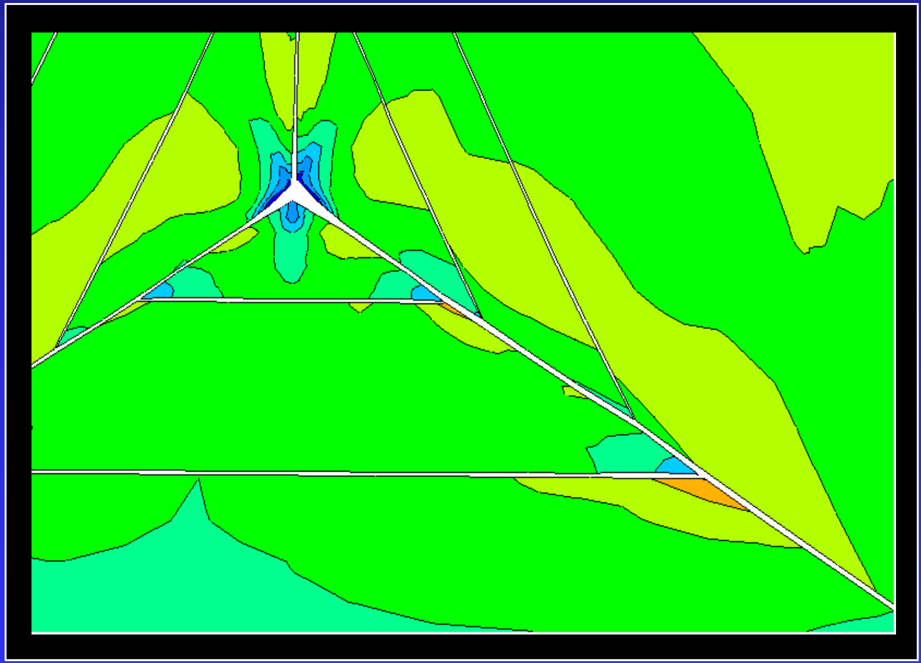

Results Contd.

Around 3-Colony Junction

$\varepsilon=0.0319$

With Lamellar Interfaces

Equivalent Plastic Strain	Hydrostatic Stress
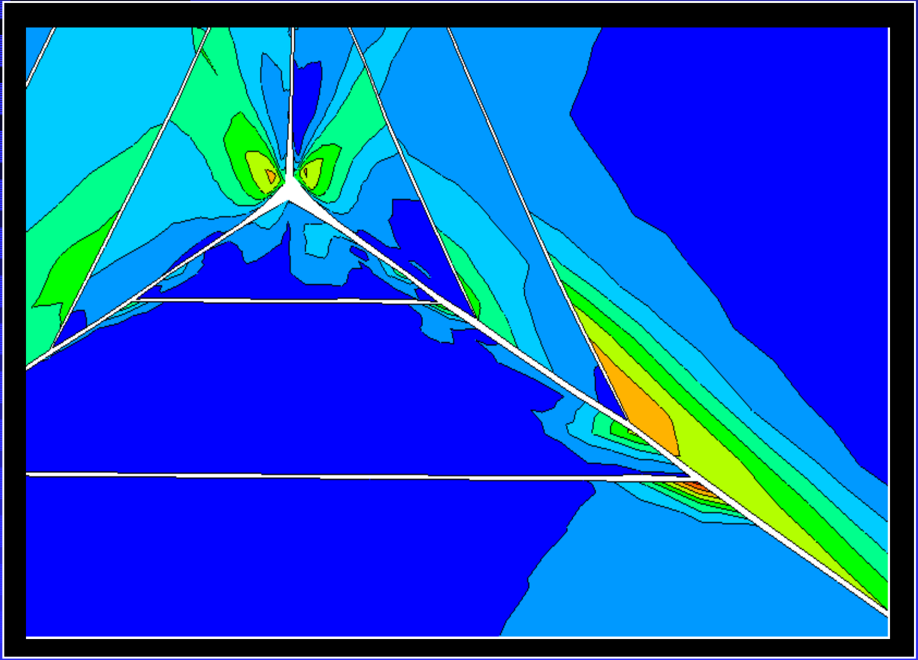	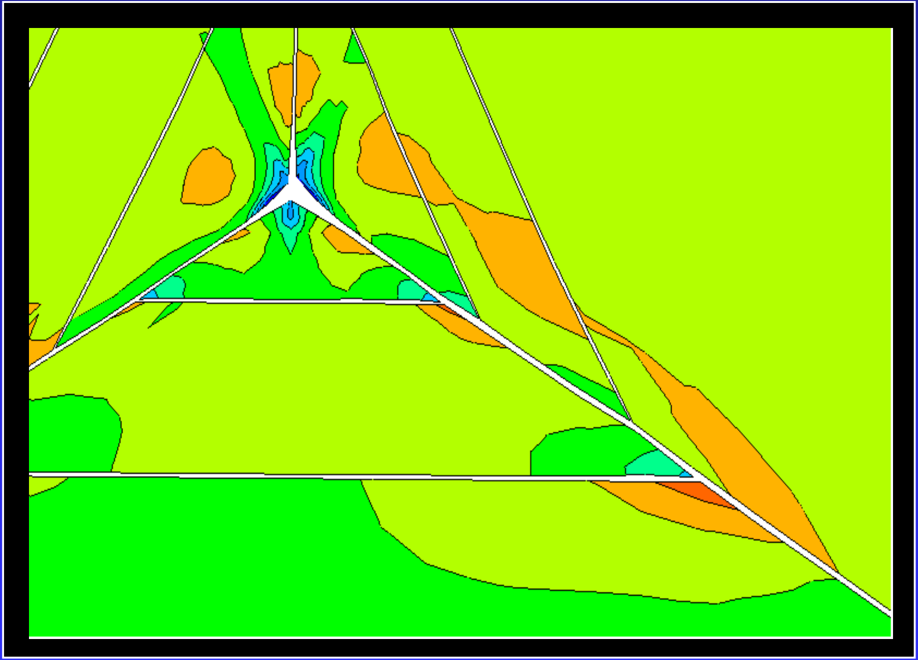

Results Contd.

Normal Stress Vs Normal Strain

y-Direction

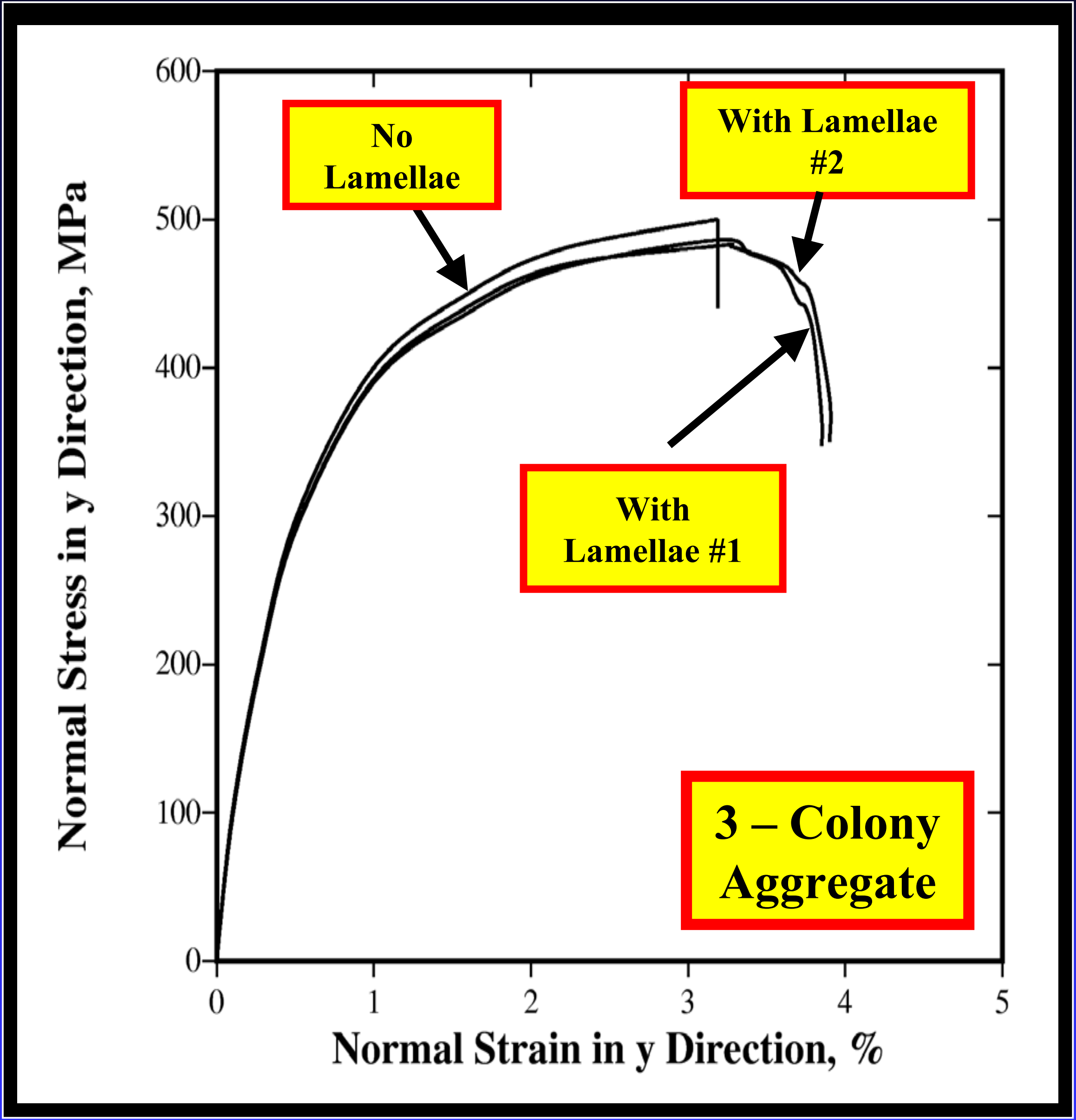

Conclusions

Conclusions

• Crystal Plasticity can reasonably well account for deformation behavior of γ-TiAl and α_2-Ti_3Al Single Crystals as well as γ-TiAl + α_2-Ti_3Al Polysynthetically-Twinned Single Crystals.

• Deformation Behavior in Polysynthetically Twinned Single and Polycrystalline γ-TiAl + α_2-Ti_3Al alloys is Dominated by Soft-Mode Slip in γ-TiAl and Hard-Mode Slip in α_2-Ti_3Al.

• Plastic Flow Incompatibilities Near Some Three-Colony Junctions Gives Rise to Tensile Hydrostatic Stresses and Inter-Colony Fracture.

• Presence of Interlamellar Boundaries in Colonies Leads to Delocalization of Fracture and in Turn, to a Higher Damage Resistance of the Material.

• Good Agreement With Experiments Relative to the Role of lamellar and Colony Boundaries on Fracture Toughness and Initiation of Fracture.

END